Final report on in-reactor tensile tests on OFHC - Copper and CuCrZr alloy

Singh, B.N; Edwards, D.J.; Tähtinen, S.; Moilanen, P.; Jacquet, P.; Dekeyser, J.

Publication date:
2004

Document Version
Publisher's PDF, also known as Version of record

RISØ

Risø-R-1481(EN)

Final Report on In-Reactor Tensile Tests on OFHC –Copper and CuCrZr Alloy

B.N. Singh, D.J. Edwards, S. Tähtinen,

P. Moilanen, P. Jacquet and J. Dekeyser

Risø National Laboratory
Roskilde
Denmark
October 2004

Authors: B.N. Singh[1)], D.J. Edwards[2)], S. Tähtinen[3)], P. Moilanen[3)],P. Jacquet[4)] and J. Dekeyser[4)]
Title: Final Report on In-Reactor Tensile Tests on OFHC –Copper and CuCrZr Alloy
Department: Materials Research Department

[1)]Materials Research Department, Risø National Laboratory
DK-4000 Roskilde, Denmark

[2)]Materials Structure and Performance Group, Pacific
Northwest National Laboratory, Richland, WA 99352, USA

[3)]VTT Industrial Systems
FIN-02044 VTT, Finland

[4)]Reactor Experiments Department
SCK.CEN
Boeretang 200, B-2400 Mol, Belgium

Risø-R-1481(EN)
October 2004

ISSN 0106-2840
ISBN 87-550-3377-6 (internet)

Contract no.: TW2-TVV-SITU (EFDA)

Groups own reg.no.:
1610013-00

Sponsorship:
EU–Fusion Technology Programme

Cover:

Abstract

At present, practically nothing is known about the dynamic response of materials subjected simultaneously to an external force and a flux of neutrons. In an endeavour to elucidate some of the essential features of the deformation behaviour under these conditions, we have recently performed a series of uniaxial tensile tests on pure copper and a CuCrZr alloy in a fission reactor at 363 and 393K. In the following, we first describe the experiments and then present results illustrating the build up of stress as a function of concurrently increasing strain and displacement dose level. Results on both pre- and post-deformation microstructures determined on the unirradiated as well as irradiated specimens using transmission electron microscopy (TEM) are also presented.

In these experiments, the transition from elastic to plastic regime occurs without any transient such as yield drop. As a result of the combination of strain and radiation hardening, the rate of hardening in the plastic regime is found to be enhanced. The rate of hardening, the maximum level of hardening and the magnitude of the total elongation achieved during an in-reactor test are found to depend strongly on the pre-yield dose level (i.e. the level of the neutron fluence received by the material prior to the on set of plastic deformation). Dislocation activities in these experiments are significantly reduced compared to that in the case of the deformation of unirradiated materials. Even in the absence of a yield drop, the plastic deformation is found to be localized in the form of cleared channels. The phenomenon of cleared channel formation also appears to be affected by the pre-yield dose level. The evolution of these channels appears to control the uniform elongation and the lifetime of the specimens. The main implications of these results are briefly discussed.

Pages: 47
Tabels: 3
References: 12

Risø National Laboratory
Information Service Department
P.O. Box 49
DK-4000 Roskilde
Denmark
Telephone +45 46774004
bibl@risoe.dk
Fax +45 46774013
www.risoe.dk

Contents

1 Introduction

It has been known for a considerable period of time that the deformation behaviour of metals and alloys is substantially altered by irradiation with energetic particles such as fission or fusion neutrons, particularly at temperatures below the recovery stage V. This effect of irradiation on mechanical properties has been a subject of extensive investigations for more than 40 years (Blewitt et al. 1960, Makin 1966 and Diehl 1969). The post-irradiation deformation experiments (i.e. tensile tests) have demonstrated consistently that (a) the yield strength of metals and alloys increases with increasing dose level, (b) materials irradiated to a displacement dose beyond a certain level exhibit the phenomenon of yield drop and (c) the irradiation causes almost a complete loss of work hardening ability and a drastic reduction in the uniform elongation (i.e. ductility). Under these conditions, in many cases the specimens show a clear sign of plastic instability immediately beyond the yield drop. It is interesting to note that these features are common to all three crystal structures, fcc, bcc and hcp (see Singh et al. 1997 for a review).

It is this prospect of irradiation induced drastic decrease in ductility and the possibility of initiation of plastic instability that has given rise to a serious concern regarding the mechanical performance and lifetime of materials used in structural components of a fission or a fusion reactor. In view of the seriousness of this technological concern, it is only prudent to consider the relevance of these adverse effects of neutron irradiation observed in the post-irradiation experiments to the performance of materials exposed simultaneously to an intense flux of neutrons and stresses in a real reactor environment. The reason for considering this issue of relevance is the recognition of the fact that the materials tested in the post-irradiated state respond to conditions that are fundamentally different from those that are likely to be experienced by the materials exposed to a dynamic irradiation environment in a fission or a fusion reactor.

In the case of post-irradiation experiments, for example, the samples are first irradiated in unstressed condition to a certain displacement dose level to accumulate a certain amount of displacement damage in the form of defect clusters (which are responsible for hardening and reduction in ductility). This means that the damage accumulation takes place in the absence of deformation-induced mobile dislocations. The irradiated samples are then tensile tested outside of the reactor, i.e. in the absence of continuous production of defect clusters. The materials employed in the structural components of a fission or a fusion reactor, on the other hand, will be exposed simultaneously to internal and external stresses and irradiation-induced defects and their clusters continuously produced during irradiation. Under these conditions, both the magnitude and the spatial distribution of defect accumulation and hence the deformation behaviour may be significantly different from that in the case of post-irradiation experiments (see later for further details). It is, therefore, relevant to consider as to whether or not the results and the conclusions of the post-irradiation deformation experiments can be taken to represent the behaviour of materials employed in the structural components of a fission or a fusion reactor. In our view, this question can be answered properly and reliably only by determining experimentally the deformation behaviour of materials in the neutron environment of a nuclear reactor. Recently, we have performed a series of such deformation experiments in the BR-2 reactor at Mol (Belgium) and have determined the dynamic stress-strain curves for pure copper and a CuCrZr alloy at 363 and 393 K. In the following we first

describe briefly the whole experimental facility designed and constructed to carry out in-reactor tensile tests (section 2). The results obtained are described in section 3. The present results and observations are briefly discussed in section 4. Section 5 presents a summary of the main results and some preliminary conclusions.

2 Materials and Experimental Procedure

2.1 Materials

The material used in the present investigation was thin (0.3 mm) sheet of oxygen-free high conductivity (OFHC) copper containing 10, 3, <1 ppm and <1 ppm, respectively, of Ag, Si, Fe and Mg. The oxygen content of this copper was found to be 34 appm. Tensile samples of polycrystalline OFHC-copper (see figure 1 for size and geometry) were annealed at 823 K for 2h in a vacuum of 10^{-9} bar. The resulting grain size and dislocation density were about 30 μm and $\leq 10^{12}$ m^{-2}, respectively. These annealed specimens were used in the in-reactor uniaxial tensile tests performed in the BR-2 reactor at Mol (Belgium).

The CuCrZr (Cu-0.73 Cr, 0.14% Zr) alloy supplied by Outokumpu Oyj (Finland) was solution annealed at 1233K for 3h, water quenched and then prime-aged at 733K for 3h. After prime ageing, the specimens were further annealed in vacuum at 873K for 1h and then water quenched. This heat treatment was given to coarsen the precipitates and yielded a microstructure containing small Cr-rich precipitates with an average size of 8.7 nm and density of $1.7x10^{22}$ m^{-3} (see Singh et al. 2004).The final grain size was found to be ~60 μm. Specimens with this final heat-treatment were used for the in-reactor tensile tests at 393K.

2.2 Test module and irradiation rig

In order to carry out these tensile experiments, a special test facility consisting of a pneumatic tensile test module and a servo-controlled pressure adjusting loop was designed and constructed. The pressure adjusting loop operates on a continuous flow of helium gas through an electrically controlled servo valve.

The basic principle of the tensile test module is based on the use of a pneumatic bellow to introduce stress and a linear variable differential transformer (LVDT) sensor to measure the resulting displacement produced in the tensile specimen. The movement of the bellows is controlled by LVDT sensor which also gives the feedback signal for the servo controller. The outside diameter of the module is 25 mm and the total length of the module together with the LVDT is 150 mm. A special calibration device was used to calibrate the applied gas pressure in the bellow with the actual load acting on the tensile specimen. A two-step calibration procedure was implemented where in the first step the characteristic stiffness of the bellow together with friction forces of the moving parts of the module were determined and in the second step the load induced on the tensile specimen by the applied gas pressure was measured directly by a load cell. The accuracy of the load calibration is approximately ± 1 % of the actual value of the stress resulting from the applied pressure causing the displacement in the specimen up to 1.3 mm. The tensile test was performed under a constant displacement rate where the servo controller compares the actual LVDT signal to the set value and close/open the servo valve to induce the movement of the bellow by increasing/decreasing the bellow pressure. Detail

of the tensile test module, calibration procedure and results are described in Moilanen and Tähtinen (2003), Singh et al. (2003), and Moilanen et al. (2004).

A number of modules were extensively tested for their functional performance and reliability before finalizing the design. The detailed design and geometry of the module was then adjusted to make it compatible with the irradiation conditions in the BR-2 reactor (i.e. the geometrical, neutronic, thermal and cooling environment).

To accommodate the test module and the necessary instrumentation to perform the uniaxial tensile test in the reactor, special irradiation rigs were designed and constructed at Mol. Figure 2a shows the simplified layout and operational features of the test module including the instrumentation. The photograh in Fig. 2b shows the final assembly of the test module, specimens and the necessary instrumentation. The whole assembly is loaded in the irradiation rig which is hung in a thimble tube. During irradiation the whole test assembly including the module and the specimens remained submerged in stagnant demineralised water. The temperature profile in each module was measured by three thermocouples placed at different positions (LVDT, specimen, bellows) in the rig (see figure 2a). Three dosimeters were placed at the specimen level to measure the neutron fluence.

2.3 In-reactor uniaxial tensile test

The irradiation rig was designed to accommodate two complete test modules such that two independent tensile tests can be performed at the same time. In addition, a tensile specimen was attached to each test module which was irradiated in unstressed condition but with the same neutron flux and at the same temperature as for the in-reactor tensile test specimen. These specimens were used for the post-irradiation (out of reactor) tensile tests and microstructural investigations in the as-irradiated and post-irradiation deformed conditions. These specimens will be referred to as “reference” specimens.

In the first in-reactor deformation experiment, two test modules were loaded in the irradiation rig. The rig was manually inserted into the open tube at position G60 of the BR-2 reactor core during the steady state operation of the reactor. As the rig was lowered in the open tube, the temperature of the test modules increased rapidly due to a gamma heating power of 4.4 Wg^{-1} and the stagnant reactor pool water close to test specimens reached an equilibrium temperature of about 363K within a couple of minutes. Note that the test temperature of each test module and the specimen was measured and recorded separately. The test specimens were not loaded during this temperature transient. Both test specimens (and the corresponding reference specimens attached to each module) received a neutron flux of 1.7×10^{17} n/m^2s ($E > 1$ MeV) corresponding to a displacement damage rate of 4.2×10^{-8} dpa/s (NRT displacement per atom).

The first in-reactor uniaxial tensile test (henceforth referred to as Test No. 1) was started about 5.5 hours after the rig was inserted in the reactor core. In other words, the tensile specimen received a displacement dose of 8.1×10^{-4} dpa while it was still without any load. The tensile test was carried out at a constant strain rate of 1.3×10^{-7} s^{-1}. This rather low strain rate was chosen to ensure that the specimen should survive the in-reactor deformation for long enough time to accumulate a displacement dose level of about 0.1 dpa. This was considered to be necessary to assess the dynamic effects of irradiation and the applied stress on the deformation behaviour of the specimen. During the test, the movement of the bellow (i.e. extension of the specimen) was measured continuously with the LVDT sensor.

The second in-reactor tensile test on the specimen in the second test module (henceforth referred to as Test No. 2) was started about 50 hours after the rig was inserted in the reactor core. In other words, the specimen accumulated displacement damage at the test temperature of 363K to a dose level of 8.3×10^{-3} dpa without experiencing any applied stress. The test was carried out with a strain rate of 1.3×10^{-7} s^{-1} and a damage rate of 4.2×10^{-8} dpa/s.

The Test No. 3 was carried out some months later as a part of another series of experiments. However, the test modules and the irradiation rig were identical to the ones used for the Tests No. 1 and 2. The tensile specimens were loaded in the same manner as described before. The irradiation rig loaded with two test modules was inserted in the same open tube as position G60 of the BR-2 reactor core during the steady state operation of the reactor. However, during this test, the test temperature equilibriated at 393K and remained almost constant during the whole test period. The stress, strain and the test temperature were measured and recorded in the same manner as for the Tests No. 1 and 2. The test was carried out with a strain rate of 1.0×10^{-7} s^{-1} and at a displacement damage rate of 5.3×10^{-8} dpa/s. There was, however, one very significant difference between this test and Tests No. 1 and 2. In this test (Test No. 3) the specimen was loaded very rapidly and the tensile test was started already only about 6 minutes after the rig was inserted in the reactor core. This means that the specimen accumulated displacement damage at 393K in the absence of applied stress only for about 6 minutes (i.e. 1.9×10^{-5} dpa). The plastic deformation during this test did not start, however, until 3.9h (i.e. 7.5×10^{-4} dpa) after the start of the test.

The specimen in the test No. 3 survived the whole reactor period and yielded a homogeneous strain of 14.2%. This measured strain value is in agreement with the strain value estimated from the measured gauge width and thickness before and after the in-reactor tensile test. After about 6% of strain, the stress measuring facility developed some faults and the stress measurements beyond the strain level of about 6% became erratic and unreliable. The total displacement dose accumulated during this test was 0.074 dpa.

One of the test modules in the second series of the in-reactor tests was loaded with a tensile specimen of prime and overaged CuCrZr alloy. The test (Test No. 4) was performed at 393K and a strain rate of 1.0×10^{-7} s^{-1}. The displacement damage rate was $\sim 5.3 \times 10^{-8}$ dpa s^{-1}. The test was started about 8 minutes after the test assembly was installed in the reactor. In other words, the specimen received a displacement dose of $\sim 2.6 \times 10^{-5}$ dpa in the absence of applied stress. It took about 14.4 hours ($\sim 2.1 \times 10^{-3}$ dpa) to reach the yield stress (i.e. the initiation of plastic deformation). The test was terminated after about 196 hours (3.7×10^{-2} dpa) of irradiation and test time. It should be noted that the specimen remained in the reactor and continued to receive neutron flux until the irradiation rig containing Test No. 3 and Test No. 4 was taken out of the reactor after 390h (0.074 dpa).

2.4 Microstructural Investigations

The microstructure of samples in various states (e.g. unirradiated and deformed, as-irradiated, irradiated and deformed and in-reactor deformed) was investigated using a JEOL 2000FX transmission electron microscope (TEM). Thin foils for TEM examination were prepared by twin-jet electropolishing in a solution of 25% perchloric acid, 25% ethanol and 50% water at 11 V and 9.5 mA for about 15 s at ~293 K. Prior to electropolishing, the TEM discs were mechanically polished down to a thickness of ~120 μm. For the investigation of the post-deformation microstructure, 3 mm discs were

punched out of the gauge length of tensile specimens. In cases where specimens had fractured (e.g. during post-irradiation tests) or cracked (e.g. during the in-reactor Test No. 1, 2 and 4), discs were punched out from the portion of the gauge length closest to the fractured or cracked surface.

3 Experimental Results

Before presenting the actual results of the in-reactor tensile tests it is only appropriate to clarify the experimental conditions under which the materials response has been determined. Furthermore, this clarification is crucially important in order to understand and appreciate fundamental differences between the traditional post-irradiation tensile tests and the present in-reactor tensile tests. The post-irradiation tensile test is performed, for instance, on a specimen which has been already irradiated (in the absence of any applied stress) at a certain temperature and to a certain displacement dose level but in the absence of applied stress. In other words, the specimen, prior to the commencement of the tensile test has a given defect microstructure which has evolved in response to the irradiation temperature and the dose level but in the absence of applied stress. The stress-strain response measured during a post-irradiation test must reflect, therefore, the deformation behaviour of the “frozen-in” irradiation-induced microstructure.

In the case of the in-reactor tensile test, on the other hand, the situation is entirely different. Here, the tensile specimen is loaded in the fully annealed condition and begins to deform when it has a relatively low density of irradiation-induced defect clusters. Hence, the material will begin to deform in a manner similar to the unirradiated virgin material with a characteristic low yield stress. However, as test continues with a constant damage rate and strain rate, the density of both the irradiation-induced clusters (interstitial loops and clusters and vacancy SFTs) and deformation-induced dislocations will increase with increasing displacement dose (and strain). In other words, the measured stress response in these experiments includes the time (i.e. dose) dependence of both work hardening and radiation hardening.

It is important to note here that for practical reasons (see section 2.3) it was not possible to apply the external load on the specimens immediately after they were exposed to neutrons in the reactor. The procedure of loading the specimens to activate the in-reactor tensile tests always took some finite time. Consequently, specimens used in all the four in-reactor tests (i.e. Test No. 1 – 4) received a different amount of displacement dose before experiencing the applied stress (henceforth referred to as pre-loading dose). This pre-loading dose affects the yield stress such that the higher the pre-loading dose, the higher is the yield stress. This means that during the in-reactor test at a constant strain rate, the specimen with a higher pre-loading dose (and a higher yield stress) remains in the elastic deformation regime for a longer time and receives a higher amount of displacement dose before the specimen reaches the yield stress and starts generating dislocations. This dose level is defined as pre-yield dose (see Table 1).

3.1 Mechanical response

As indicated earlier, during in-reactor tensile testing, a specimen experiences simultaneously an externally applied stress and a flux of neutron-induced defects and defect clusters. It is of interest, therefore, to examine first of all the measured raw results on the build up of stress and strain in the specimens as a function of irradiation (and tensile test) time. Results for three such in-reactor tensile tests on pure copper are shown

in figure 3 for the irradiation and test temperatures of 363K (Test No. 1 and 2) and 393K (Test No. 3). As can be seen in figure 3, the actual tensile test on these specimens were initiated at three different times after the specimens were brought in the reactor. In other words, the specimens in Test No. 1, 2 and 3 received different levels of displacement doses (see Table 1) while they were still at zero stress. Doses at which the yield point was observed and at which the tensile test was discontinued are also given in Table 1. The tensile properties of un-irradiated, post-irradiated and in-reactor tensile tested specimens at 363 and 393K are summarised in Table 2. The results presented in figure 3 clearly illustrate that the temporal evolution of the stress response of the material under the dynamic testing conditions is significantly affected for the whole lifetime of the test by the pre-loading displacement dose level. It is self-evident from the results that it is not only the yield strength but also the maximum level of hardening and the total elongation (i.e. lifetime) of the material are noticeably dependent on the level of pre-loading displacement dose level. It is rather surprising that even a pre-loading dose level of only 1.5×10^{-5} dpa (see Table 1) significantly alters the stress response of the material (Test No. 3, figure 3). It should be mentioned here that the influence of the pre-loading dose levels on the microstructural response is described in section 3.2.

In order to make the raw results of the in-reactor tests comparable with the conventional tensile test results, we have transformed the raw results presented in figure 3 into conventional stress-strain curves and the results are shown in figure 4. This transformation is straightforward since the tests are performed at a constant strain rate which is continuously measured during each test. For comparison purposes, the stress-strain curves for the unirradiated as well as post-irradiated copper specimens tested at the irradiation temperatures are also shown in figure 4. Of course, both the unirradiated and post-irradiated specimens were tensile tested outside of a reactor and at two different strain rates. It is worth noting here that the specimens used in the post-irradiation tests were irradiated in the same test module used for the in-reactor Test No. 1, 2 and 3 (see section 2.3 and Table 1)

The results presented in figure 4 illustrate the following significant differences in the effect of irradiation on the mechanical response between the conventional post-irradiation tensile tests and the dynamic in-reactor tensile tests:

(i) The post-irradiation test of specimens irradiated at 363K even to a dose level of as low as 0.047 dpa exhibits the occurrence of a yield drop showing a clear transient between the elastic and plastic deformation regime. In the case of the in-reactor Test Nos. 1 and 3, on the other hand, there is no indication of such a transient. It is interesting to note though that in the case of the Test No. 2 which was given a pre-loading irradiation to a dose level of only 8.3×10^{-3} dpa, the stress-strain curve does, in fact, show a tendency for the occurrence of such a transient.

(ii) The post-yield hardening behaviour in the post-irradiation tensile test is also distinctly different from that in the case of in-reactor tests. Although the rate of hardening is clearly higher in the in-reactor tests, yet the level of maximum hardening (i.e. ultimate tensile strength) remains significantly lower than that in the post-irradiation tests.

(iii) In the case of the in-reactor tensile tests, both the yield stress and the level of the maximum hardening are dependent on the pre-loading displacement dose level. The lower this dose level, the lower is the yield stress as well as the maximum hardening.

(iv) The uniform elongation measured in the in-reactor tests is dependent on the pre-loading dose level. The lower the pre-loading dose level, the larger is the uniform elongation.

The results of post-irradiation tensile tests on neutron irradiated copper at temperatures in the range of 300 – 473 K (Zinkle and Gibson 1999) have consistently shown that the yield stress increases with increasing displacement dose level, reaching a saturation level at ~0.1 dpa. The dose dependence of the yield stress determined from the present in-reactor as well as post-irradiation tensile tests at 363 and 393 K is shown in figure 5. The results of an earlier series of post-irradiation experiments on the same OFHC-copper neutron irradiated (at a very similar damage rate as in the present work) and tested at 373 K (Singh et al. 2001) are also plotted in figure 5. The fact that the dose dependence obtained from the in-reactor tests is reasonably consistent with the results of the post-irradiation tensile tests can be interpreted to mean that the in-reactor tests are justifiably valid tensile tests.

While considering the effect of irradiation on the deformation behaviour of metals and alloys, it is worth recognizing that our current knowledge of this effect is based exclusively on the results of post-irradiation tensile tests. Traditionally, the magnitude of the effect is evaluated in terms of the dose dependence of the increase in the yield stress, $\Delta\sigma_y$, due to irradiation. The magnitude of the $\Delta\sigma_y$ is obtained simply by subtracting the yield stress of the unirradiated specimen from that of the post-irradiation yield stress at a given dose level (see figure 5). Although it has been well known that the work hardening ability of the irradiated material during post-irradiation tensile tests is considerably reduced, the effect of irradiation on the flow stress in the post-yield deformation regime has not been , to our knowledge, properly evaluated.

In the case of the in-reactor tensile tests, on the other hand, in order to understand the dynamic nature of the combined effects of the applied stress and displacement damage, it is necessary to evaluate the hardening behaviour as a function of irradiation and test time (i.e. concurrently accumulating displacement dose and plastic strain). In other words, we need to determine the effect of irradiation not only on the yield stress but also on the hardening behaviour (i.e. the flow stress) in the post-yield deformation regime as a function of both displacement dose level and plastic strain. To facilitate such analyses, we first present the true stress – true strain curves for the in-reactor tensile tests in figure 6(a). Figure 6(b) shows the true stress – true strain curves for the corresponding post-irradiation tests carried out at 363 and 393 K. The true stress – true strain curves for the unirradiated reference specimens tested at 363 and 393 K are also shown in figures 6(a) and 6(b).

The effect of irradiation on the increase in the yield stress, $\Delta\sigma_y$, and the flow stress, $\Delta\sigma_f$, is obtained directly from the results presented in figures 6(a) and 6(b). The dose dependence of both $\Delta\sigma_y$ and $\Delta\sigma_f$ is presented in figure 7 for the in-reactor tests carried out at 363 and 393K. Clearly, the dose dependence of the increase in the yield stress is significantly stronger than that of the increase in the flow stress. Furthermore, the increase in the flow stress in Tests No. 1 and 3 has tendency to reach a saturation level and this saturation level is strongly influenced by the pre-loading displacement dose level.

The effect of irradiation on the hardening behaviour in the post-yield deformation regime (i.e. increase in the flow stress, $\Delta\sigma_f$, due to irradiation and deformation) for the in-reactor tensile tests is shown in figure 8 as a function of true plastic strain. Note that these results are obtained from the results shown in figure 6(a).

The following aspects of the results shown in figure 8 regarding the "strain hardening"* behaviour during in-reactor tests should be noted:

(a) The rate of strain hardening increases with decreasing pre-loading dose level,

(b) The strain hardening rate during a given test decreases with increasing plastic strain and seems to saturate at a certain strain level,

(c) Both the saturation level and the plastic strain at which the saturation in the strain hardening occurs decrease with decreasing pre-loading dose level.

The engineering stress-strain curve for the in-reactor Test No. 4 on CuCrZr specimen is shown in figure 9. The stress-strain curve was constructed from the raw data collected continuously during the in-reactor test in terms of the stress response as a function of irradiation and tensile test time, as shown in figure 3 for Tests No. 1, 2 and 3. For comparison, the stress-strain curves for specimens tested out of pile at 393K in the un-irradiated and post-irradiation conditions are also shown in figure 9. The specimen used for the post-irradiation test was irradiated in the same test module used for the in-reactor Test No. 4 at 393K. Note that the post-irradiated specimens received a displacement dose of 0.074 dpa.

The stress-strain curve for the in-reactor Test No. 4 (figure 9) demonstrates that, like in the case of pure copper, the plastic deformation even in the CuCrZr specimen occurs in a homogeneous fashion and without any transient in the form of a yield drop. It is interesting to note, however, that the level of increase in the hardening in CuCrZr due to irradiation is far less than that in the case of pure copper and comes to saturate at a much lower dose (strain) level. Soon after reaching the saturation level, the specimen begins to neck which leads to the initiation of fracture. Consequently, the specimen yields a uniform elongation of only about 5% (see Table 2).

Figure 10 shows the true stress – true strain curves corresponding to the curves shown in figure 9. In order to illustrate the effect of irradiation on the hardening behaviour in the post-yield deformation regime, the change in the flow stress, $\Delta\sigma_f$, due to irradiation is plotted in figure 11 as a function of true plastic strain. For comparison, the variation of $\Delta\sigma_f$ with strain for the test No. 1 on copper (figure 8) at 363K is also shown in figure 11. Note that the pre-yield dose in Test No. 1 is very similar to that in the Test No. 4 (see Table 1). It is rather interesting to note that the strain hardening in the case of CuCrZr specimen reaches a maximum and then decreases with increasing strain (dose) indicating onset of dynamic softening. This behaviour is clearly different from what is observed in the case of pure copper.

3.2 Microstructural response

In order to help understand the mechanical response of the specimens determined during in-reactor tensile tests, different aspects of physical and microstructural changes due to deformation under irradiation have been investigated. In the following, we shall first describe the irradiation and deformation induced physical changes such as formation and propagation of cracks and dimensional changes in the gauge section of tensile specimens after they were taken out of reactor. This will be followed by the result of TEM investigations of defect clusters (e.g. loops and stacking fault tetrahedra (SFT_s)), dislocations and cleared channels present in the specimens after the completion of tensile tests and irradiation.

---

*) Refers to hardening due to deformation as well as irradiation.

3.2.1 Physical state of specimens after in-reactor deformation

Figure 12 shows photographs of the in-reactor tensile tested specimens of copper and CuCrZr alloy after they were taken out of the reactor and refer to the in-reactor test (a) No. 1, (b) No. 2 (c) No. 3 and (d) No. 4 (see section 2.3 for details). The specimens in Test No. 1 and 2 yielded a total elongation of 13 and 8%, respectively (see Table 2). The tensile specimen used in Test No. 3 was removed from the reactor (at the end of the reactor period) after a total strain of 14% (Table 2). The CuCrZr specimen used in the Test No. 4 yielded a total elongation of only about 7% (Table 2).

First of all, it should be noted that in all four cases shown in figure 12, the edges of the gauge section of the tensile specimens remained straight and parallel showing that no noticeable necking had occurred during the in-reactor tests. This directly implies that the deformation in all cases has occurred in a homogeneous fashion. This is consistent with the smooth nature of the stress-strain curves shown in figure 4. This is also consistent with the dislocation microstructure observed in these specimens (see later).

Another significant piece of information emerging from the photographs shown in figure 12 is that the specimens from Test No. 1, 2 and 4 show clear evidence of crack initiation and propagation. There is, on the other hand, absolutely no indication of crack initiation in the specimen used in the Test No. 3 even though this specimen has been deforming for the longest period of time and to a total elongation of 14% before the test was discontinued. Furthermore, it is interesting to note that the crack in the specimen from the Test No. 2 seems to be deeper and more advanced than that in the specimen from the test No. 1 even though the former has been under stress for a shorter time and has yielded a smaller elongation than the latter. To examine this difference further, both specimens (i.e. from the Tests No. 1 and 2) were polished from both sides of the gauge thickness down to a final thickness of ~120 μm. Figure 13 shows optical micrographs of both sides of the polished specimens from the Test No. 1 (figure 13a, b) and from Test No. 2 (figure 13c,d). Clearly, it is evident that in the specimen from Test No. 2, the crack has penetrated through the whole thickness of the specimen and has advanced through almost across the whole gauge width of the specimen. In the case of the specimen from the Test No. 1, on the other hand, the crack appears to remain rather localized and shallow and has not penetrated through the thickness of the specimen.

The observations described above illustrate that although all specimens representing Tests No. 1, 2, 3 and 4 deform homogeneously, yet their lifetime (i.e. total elongation before crack initiation) varies significantly among these tests. The results also suggest that these differences in the lifetime may arise from the differences in the initiation and growth behaviour of cracks among these specimens. The origin of these differences will be discussed in section 4.

3.2.2 Post-deformation microstructure of unirradiated specimens

In an effort to clarify the effect of irradiation on the evolution of dislocation microstructure during deformation in the in-reactor tensile tests, unirradiated and annealed (550^{o}C/2 h) reference specimens of copper were tensile tested outside the reactor. Tests were performed using the same test module, strain rate and test temperature as that used in the in-reactor tensile tests. In these tests, the specimens were strained up to a certain strain level and then the test was interrupted. The specimen was taken out of the test module for TEM examinations. Specimens strained to total strain levels of 4 and 20% were investigated.

The dislocation microstructure of specimens deformed to 4 and 20% total elongations are shown in figures 14(a) and 14(b), respectively. The main feature of the microstructure is that the motion and interaction of dislocations generated during deformation lead to this segregation in the form of dislocation walls and cells of dislocation walls already at the strain level of 4%. Practically no isolated individual dislocations are observed within the cells (figure 14(a)). At the strain level of 20%, the essential features of the dislocation microstructure remain the same as that at 4% strain. The main difference in the microstructure between these two cases is that the dislocation walls are somewhat thicker and contains more dislocations in the case of 20% deformed specimens than that in the case of 4% deformation (figure 14(b)). In the case of 20% deformation, it can be seen in figure 14(b) that some of the dislocation cells have subdivided into smaller ones. The observed microstructure is consistent with the stress-strain curve shown in figure 4.

3.2.3 Characterization of irradiation induced interstitial and vacancy clusters

The evolution of irradiation induced clusters of self-interstitial atom (SIAs) and vacancies in the form of loops and stacking fault tetrahedra (SFT_s), respectively, in neutron irradiated copper is well known (e.g. Singh and Zinkle 1993, Singh et al. 2001). What is not known, however, is the evolution of these clusters when the damage accumulation occurs under the condition of concurrent generation of defects and their clusters by neutrons and of the mobile dislocations by the applied stress. Since freshly generated mobile dislocations are likely to interact with glissile as well as sessile clusters produced continuously by cascades, both the defect accumulation and the radiation hardening behaviour of the material may be different from what is commonly observed in the post-irradiation deformation experiments. In order to understand the deformation behaviour of specimens during the in-reactor tensile tests, it is, therefore, important to determine the details of defect cluster and dislocation microstructures that evolve during these tests. In this section we first describe the results on the defect clusters and the results on the dislocation microstructure is described in the next section (3.2.4).

To illustrate the effect of stress on the microstructural evolution during irradiation, the defect microstructure of the “Reference” specimens (irradiated without stress, see section 2.3) is shown in figure 15. Figures 15(a) and (b) show the loop microstructure in the “Reference” specimens in the as-irradiated condition for the irradiation temperatures of 363 and 393K, respectively. It should be pointed out that in addition to the presence of small and isolated SIA loops, both figures 15(a) and (b) show the tendency for the formation of “raft” like microstructure. Formation of such raft-like structure of SIAs in OFHC-copper have been reported earlier for the irradiation temperature of 373K and a dose level of 0.1 dpa (Singh et al. 2001).

The size distributions of SFT_s for the reference specimens (without applied stress) used in the Tests No. 1 and 2 irradiated at 363K are shown in figure 16. As can be seen in figure 16, the two reference specimens yield almost identical results. These results are also very similar to the one reported earlier for irradiation at 373K (Singh et al. 2001).

Figure 17 compares the size distributions of SFT_s for the reference (unstrained) and the strained (in the reactor) specimens irradiated and deformed at 363K to 13% uniform strain. For TEM investigations, discs were prepared of materials taken from near the crack in both strained specimens. In the case of specimen strained to 13% strain, the density of SFT_s smaller than ~2.5 nm is noticeably lower than that in the reference specimen. The density of SFT_s larger than ~3.0 nm is almost the same in reference

(unstrained) and 13% strained specimens (figure 17). The total SFT density in the strained (13%) specimen was found to be lower than that in the reference specimen.

3.2.4 Dislocations and cleared channels in the in-reactor deformed specimens

Before describing the microstructure of the in-reactor deformed specimens, it should be pointed out that the results reported in the following represents the final microstructure at the end of the in-reactor deformation experiments. In other words, the nature of the temporal evolution of the microstructure under these conditions remains unknown and can be only deduced. In this section we first report the dislocation microstructure observed at the end of the in-reactor tensile tests. This is then followed by the results on the formation of cleared channels.

Dislocation Microstructure

Figure 18 shows a representative example of the microstructure observed in the TEM discs taken from the region close to the crack in the tensile specimen used in the Test No. 1 (see figure 9a). It is worth recalling that this specimen has experienced 13% of homogeneous plastic deformation prior to the appearance of crack when the loading was discontinued and the specimen was taken out of the reactor (see section 3.2.1). The visible microstructure shows fairly homogeneous distribution of dislocation segments, black dots which are most probably SIA clusters and some loop like structure (which is expected to be of interstitial type). The presence of the high density of small SFT_s in this specimen (see figure 17) is not visible in this relatively low magnification micrograph shown in figure 18. It is interesting to note that practically all dislocation segments are curved and show some limited amount of movement. However, there is no indication of any extensive dislocation motion and dislocation-dislocation interactions, causing segregation of dislocations in the form of dislocation walls. This is in a dramatic contrast to dislocation behaviour observed in the specimens deformed in the unirradiated condition (see figure 14). The microstructure shown in figure 18 is also significantly different from that commonly observed in the post-irradiation deformation experiments. In these investigations, the specimens irradiated and subsequently tensile tested at temperatures in the range of ~300 – 373K to doses of >0.01 dpa show no evidence of global generation of dislocations from F-R sources (see Singh et al. 1995, 2001). During the post-irradiation deformation dislocations are generated only at the regions of stress/strain concentration (e.g. boundaries and interfaces). These dislocations are responsible for the formation of cleared channels (see later for discussion).

The microstructure of the specimen deformed in the in-reactor Test No. 2 is shown in figure 19. Like in the previous case (i.e. Test No. 1), the TEM disc was taken from the region close to the crack in the tensile specimen (see figure 9b). The general features of the microstructure are very similar to those exhibited by the in-reactor tested specimen in the Test No. 1 (see figure 18). The visible (in figure 19) part of the microstructure consists of relatively short and curved dislocation segments, small clusters and loop-like features. The spatial distribution is fairly homogeneous. The specimen also contained a high density of small SFT_s (not visible in figure 19). The main significance of the microstructure is that during in-reactor tensile test a large number of dislocations are generated throughout the whole specimen but their movement remains rather limited. Consequently, dislocation-dislocation interactions and the formation of segregated features like dislocation walls do not take place. As mentioned above, these features are entirely different from the microstructure commonly observed in the unirradiated and deformed or in the post-irradiated and deformed copper.

It should be pointed out that the specimen in the Test No. 2 was irradiated for the first 50 hours without any load and then the stress was applied. Towards the end of the experiment, the specimen received neutron flux in the absence of applied stress for about 100 hours since after the initiation of a rapid drop in the stress level on the specimen, the stress was reduced to about 100 MPa. In other words, details of the microstructures for the Test No. 1 and Test No. 2 should not be directly compared.

The dislocation microstructure in the specimen used in the in-reactor Test No. 3 is shown in figure 20. Since this specimen showed no sign of crack formation (see figure 12c), the TEM disc for the microstructural investigation was taken from the centre of the gauge section of the tensile specimen. Just like in the case of Test Nos. 1 and 2, the visible microstructure is dominated by the presence of relatively short segments of dislocations and small interstitial clusters in the form of black dots. The presence of the high density of very small SFT_s are not resolved in figure 20. Once again, there is no indication of any extensive dislocation motion and interactions. This is somewhat surprising since this specimen was loaded very quickly after it was brought in the reactor. The specimen received a displacement dose of only 7.5×10^{-4} dpa before it started deforming plastically (see Table 1). It is rather significant that even such a low dose of pre-irradiation prevented the long-distance migration of dislocations and the formation of dislocation walls and cells.

Cleared Channel Formation

In the post-irradiation deformation experiments, the formation and propagation of cleared channels are the most prominent features (Edwards et al. 2004). It was, therefore, of a great interest to investigate the specimens tensile tested directly in the reactor. Even though neither the stress-strain curves (figure 4) nor the dislocation microstructure suggest the occurrence of plastic flow localization, the formation of cleared channels were observed in all four in-reactor tensile tested specimens. Examples of cleared channels observed in the specimens from Test No. 1, 2 and 3 are shown in figures 21a, 21b and 21c, respectively. The width of the channels varied between ~100 and 250 nm. It should be mentioned, however, that generally the channels in the specimen from Test No. 3 (tested at 393K) were somewhat narrower (~100 -200 nm) in width and their concentration was lower than that in the case of specimens from Test No. 1 and 2 (tested at 363K). Furthermore, the cleared channels in the specimen from Test No. 3 were rather diffused and did not appear to be in a fully developed form, indicating that they might have been formed towards the end of the test.

It is interesting to note that in the specimen from the Test No. 1 deformed in the reactor at 363K to a final dose level of 0.047 dpa, clear evidence was found of the initiation of cleared channels from twin (annealing) boundaries. An example is shown in figure 22. The channels are spaced rather regularly and are confined within the annealing twin. There is no indication of propagation of the channels across the twin boundaries into the grain. From the image shown in figure 22, it is not possible to determine as to which of the two twin boundaries has acted as the source of these channels. Such examples of channel initiation from twin boundaries have been reported recently in pure copper neutron irradiated to 0.3 dpa at 373K and post-irradiation tensile tested at 373K (Singh et al. 2004).

The propagation of a channel through the interior of a grain and across an annealing twin in the copper specimen from the in-reactor Test No. 2 at 363 K is shown in figure 23. The specimen yielded a homogeneous strain of 9% before the crack initiation occurred in the gauge section of the specimen (see figure 9b). Clearly, the interaction and

propagation of the cleared channel across the annealing twin produced very substantial damage to the twin. Both the strain concentration and the displacement at the entry as well as the exit points of the channel to and from the twin is clearly visible in figure 23. It is also of interest to note that both the formation of the cleared channel and its subsequent interaction with the twin must have taken place below a dose level of less than 3.2 x 10^{-2} dpa since the tensile loading in this experiment was discontinued at this dose level. It is worth pointing out that such interactions with similar damaging effects have been observed in post-irradiation deformation experiments but with differences that those specimens were given a much higher level of displacement dose (i.e. 0.3 dpa) (see Singh et al. 2004) and were tensile tested at a much higher strain rate (i.e. 1.3 x 10^{-3} s^{-1}).

Two thin foils were prepared from the CuCrZr specimen used in the Test No. 4 for TEM examinations. The first thin foil was from the disc taken from the outer region of the gauge length and showed no clear evidence of plastic deformation in the form of dislocations and dislocation network. Instead, the microstructure was dominated by the presence of a high density of black dot images representing small precipitates and defect clusters (figure 24a). In the second foil taken from the central region of the gauge length and the region close to where the crack had formed, the microstructure was found to be dominated by a high density of cleared channels (figure 24b). It should be pointed out that the cleaned channels do not appear to be as clean as in the case of the Test No. 1 on pure copper (see figure 18a). This may arise due to two reasons: (a) the precipitates present in the cleaned channels in CuCrZr are not completely destroyed during channel formation and (b) the specimen remained exposed to the neutron flux for more than 200 hours after these channels must have formed, (See section 2.3 and Table 1)

4 Discussion

The results presented in figures 3, 4, 6 and 10 clearly demonstrate that the deformation behaviour of OFHC-copper and CuCrZr alloy during in-reactor tests is substantionally different from that observed during post-irradiation test of specimens irradiated at temperatures below the recovery stage V. It is well established that the plastic deformation in the case of post-irradiation specimens irradiated to doses of 10^{-2} dpa or higher at temperatures below the recovery stage V is characterized by three major features: (a) a distinct transient between elastic and plastic regime in the form of a yield drop, (b) almost a complete lack of work hardening and (c) a drastically reduced uniform elongation. The results of in-reactor tests demonstrates, on the other hand, that the plastic deformation during these dynamic tests occurs in just the opposite way on all three counts mentioned above: (i) the transition from the elastic to plastic regime occurs rather smoothly (in a way very similar to the transition in the case of unirradiated copper), (ii) there is a significant amount of work hardening and (iii) the in-reactor tests yield a substantial amount of uniform elongation. In this context, it is worth noting that inspite of these differences, the dose dependence of the yield stress in the case of the in-reactor test is almost identical to that in the case of the post-irradiation tests (see figure 5). The major differences in the deformation behaviour between the in-reactor and the post-irradiation tests are summarised in Table 3.

As described in section 3.2, the microstructural evolution during the in-reactor tests is also very different from that observed in the post-irradiation tested specimens. The most significant difference is that in the specimens used in the in-reactor tests, the dislocation generation is found to occur throughout the whole specimen in a relatively homogeneous fashion. In the case of post-irradiation tested specimens, on the other hand, practically no

dislocations are generated in the volume between cleared channels. In other words, dislocations are generated only at the sites of stress/strain concentration and are responsible for the localization of the plastic flow in the form of cleared channels.

A close analysis of the mechanical response and the post-deformation microstructure of the in-reactor tested specimens reveals an interesting (from a scientific point of view) and an important (from a technological point of view) effect of the pre-loading dose level not only on the deformation behaviour but also on the lifetime (i.e. the total plastic strain prior to the initiation of failure) of specimens exposed concurrently to cascade damage and applied stress. The yield stress and the maximum flow stress of pure copper decrease with decreasing the pre-loading dose level whereas the rate of strain hardening increases with decreasing pre-loading dose level (see figures 6a and 8). The results shown in figure 7 also illustrates that the irradiation-induced increase in the flow stress comes to saturate at a lower level and at a lower displacement dose with decreasing pre-yield dose level. In other words, when the plastic deformation is induced during very early stages of irradiation, (i.e. at low levels of pre-yield dose), the effect of irradiation on hardening is considerably reduced. Consequently, the specimen under these conditions continues to deform homogeneously but without any further increase in hardening and without initiating plastic flow localization and yields a considerably higher uniform elongation (i.e. longer lifetime). This is consistent with the microstructural evidence described in section 3.2. This directly implies that the deformation behaviour of copper and copper alloys used in a component in a fusion reactor would be expected to respond in a manner similar to the response of the in-reactor tested specimens with a low level of pre-loading displacement damage. It should be pointed out, however, that this conclusion remains tenuous at least for the time being since the origin of these effects remains unclear and requires further experimental validation.

Although the deformation behaviour of the prime aged CuCrZr during in-reactor tensile test is, in many respects, very similar to that of pure copper, two significant differences should be noted. First, in the case of CuCrZr alloy, the irradiation induced increase in the flow stress reaches a maximum at a very low strain (dose) level and then begins to decrease as a function of strain (figure 11). Second, for a given pre-loading dose level, cracks are formed in the CuCrZr specimen at a much lower strain (dose) than that in the case of pure copper. The reasons for these differences are not at all clear at present. Judging from the cleared channel formation behaviour it seems plausible that both of these effects may have their origin in the factors controlling the initiation of the cleared channels.

5 Summary

The present work has clearly demonstrated the feasibility of performing well defined and controlled dynamic deformation experiments in a fission reactor. The validity of the experimental results obtained during in-reactor tensile testing has been established so that these results can be compared and contrasted with the results obtained in conventional post-irradiation tests carried out using standard mechanical testing machines outside of a reactor.

The present results obtained on OFHC-copper and CuCrZr alloy at tempera-tures in the range of 363 – 393 K have demonstrated that during the in-reactor tensile tests, the material deforms uniformly and in a homogeneous fashion. These experiments have shown no sign of yield drop and plastic instability (i.e. low-temperature embrittlement) during deformation as commonly observed during post-irradiation tensile testing.

Another important feature of the in-reactor deformation behaviour which these experiments have established is that the level of maximum hardening and the magnitude of plastic strain before the on set of fracture (i.e. the uniform elongation) are strongly dependent on the level of pre-yield displacement damage (i.e. the amount of damage accumulation in the absence of mobile dislocations generated by the applied stress). The lower the pre-yield dose, the lower is the maximum hardening and larger is the plastic strain (i.e. the higher is the uniform elongation) before the on set of fracture.

The analysis of the present results suggests that the magnitude of uniform elongation (i.e. the lifetime) for the specimens used in the in-reactor tests may be dependent on the formation and evolution of "cleared" channels. As to when these cleared channels are initiated seems to be dependent on the level of stress acting on the specimens which for a given strain level depends on the level of pre-loading displacement damage. The higher the pre-loading dose, the higher is the stress level reached at a given strain, the earlier seems to be the initiation of cleared channels leading to a lower uniform elongation and a shorter lifetime. This implies that if the tensile tests in the reactor were started instantaneously (i.e. with zero pre-loading dose) the hardening level during in-reactor testing may never reach the stress level necessary for the initiation of cleared channels. This may yield high uniform elongation. However, these interpretations remain tentative and need to be verified by appropriate experiments.

It is important to note that the deformation behaviour of CuCrZr alloy during the in-reactor tensile test is, in several respects, significantly different from that of pure copper. For the same irradiation and tensile loading conditions, the CuCrZr alloy exhibits a noticeably shorter lifetime than pure copper.

Table 1. Displacement dose levels at various stages of in-reactor tensile tests

Material	Test Number	Irradiation and Test Temperature (K)	Displacement Dose (NRT dpa) at			
			Beginning of Tensile Test[a)]	Yield Point[b)]	End of Tensile test	End of irradiation
OFHC-copper	No. 1	363	8.1×10^{-4}	2.2×10^{-3}	4.7×10^{-2}	4.7×10^{-2}
"	No. 2	363	8.3×10^{-3}	8.3×10^{-3}	3.2×10^{-2}	4.7×10^{-2}
"	No. 3	393	1.9×10^{-5}	7.5×10^{-4}	7.4×10^{-2}	7.4×10^{-2}
CuCrZr	No. 4	393	1.3×10^{-5}	2.7×10^{-3}	3.7×10^{-2}	7.4×10^{-2}

(a) and (b) refer to "pre-loading" dose and "pre-yield" dose, respectively.

Table 2. Tensile properties of unirradiated, post-irradiated and in-reactor tensile tested copper and CuCrZr specimens at 363 and 393 K

Material	Test Condition	Test No.	T_{irr} (K)	T_{test} (K)	$\dot{\varepsilon}$ (s^{-1})	σ_y (MPa)	$\sigma_{0.2}$ (MPa)	σ_{max} (MPa)	$\varepsilon_{(u)}$ (%)	$\varepsilon_{(t)}$ (%)
OFHC-copper	Unirra-diated	1 (UNR)	-	363	$1.2x10^{-3}$	32	38	162	45	49
	"	1 (UNR)	-	"	$1.3x10^{-7}$	25	31	>102[+)]	>20[+)]	>20[+)]
		3 (UNR)	-	393	$1.2x10^{-3}$	30	34	166	50	-
			-							
CuCrZr	Unirra-diated	4 (UNR)	-	393	$1.2X10^{-3}$	142	154	256	26	26
OFHC-copper	Post-irradiated	1(IRR)	363	363	$1.2x10^{-3}$	213	215	226	< 1	27
		3(IRR)	393	393	$1.2x10^{-3}$	172	178	196	<1	25
CuCrZr	Post-irradiated	4 (IRR)	393	393	$1.2x10^{-3}$	289	290	290	<1	8
OFHC-copper	In-reactor tested	1	363	363	$1.3x10^{-7}$	100	105	187	13	13
		2	363	363	"	142	142	197	8	8
		3	393	393	$1.0x10^{-7}$	56	70	-	14	14
CuCrZr	In-reactor tested	4	393	393	$1.0x10^{-7}$	169	179	225	5.5	7

(UNR) – Unirradiated Reference
(IRR) – Irradiated Reference
[+)] Test was stopped at this strain level because the design of the test module does not allow measurement of strain greater than 20%.

Table 3. Major differences in mechanical properties and post-deformation microstructure between post-irradiation and in-reactor tensile tested specimens

Post-irradiation Tests	In-reactor Tests
(i) A marked transient between elastic and plastic deformation regions in the form of a yield drop	Continuous and smooth transition
(ii) Practically no strain hardening	Strong "strain hardening"*; the lower the pre-yield dose, the stronger is the hardening rate
(iii) Because of the loss of work hardening ability, the $\Delta\sigma$ (flow) decreases with plastic strain	$\Delta\sigma_f$ increases with strain and saturates at a certain strain level. The saturated level of $\Delta\sigma_f$ decreases with decreasing level of the pre-yield dose
(iv) Lack of dislocation generation in volumes between the cleared channels	Homogeneous distribution of deformation induced dislocations between the cleared channels. No indication of dislocation-dislocation interaction and segregation of dislocations leading to the formation of dislocation walls
(v) Formation of cleared channels	Delay in the formation of cleared channels depending on the pre-yield dose level

*Refers to hardening due to deformation as well as irradiation.

Acknowledgements

The present work was partly funded by the European Fusion Technology Programme. The authors would like to thank a number of technical staff, members at Mol, VTT and Risø for their valuable help in carrying out the present experiments.

References

BLEWITT, T.H., COLTMAN, R.R., JAMISON, R.E., and REDMAN, J.K., 1960, J. Nucl. Mater., 2, 277.

DIEHL, J., 1969, in: A. Seeger, D. Schumacher, W. Schilling, J. Diehl, eds., Vacancies and Interstitials in Metals, Proc. Int. Conf. KFA Jülich, 1968 (North-Holland, Amsterdam, 1969) p. 739.

MAKIN, M.J., 1966, in: W.F. Sheely (Ed.) Radiation Effects, AIME Metallurgical Soc. Conf., Ashville, NC, September 1965, vol. 37, Gordon and Breach, New York, 1966, p. 627.

MOILANEN, P., and TÄHTINEN, S., 2003, VTT Report BTU076-031127, VTT Industrial Systems, Espoo, Finland.

MOILANEN, P., TÄHTINEN, S., SINGH, B.N., and JACQUET, P., 2004, VTT Report BTU076-031127, VTT Industrial Systems, Espoo, Finland.

SINGH, B.N., and ZINKLE, S.J., 1993, J. Nucl. Mater., 206, 212.

SINGH, B.N., EDWARDS, D.J. and TOFT, P., 2001, J. Nucl. Mater., 299, 205.

SINGH, B.N., FOREMAN, A.J.E., and TRINKAUS, H., 1997, J. Nucl. Mater., 249, 103.

SINGH, B.N., TÄHTINEN, S., MOILANEN, P., JACQUET, P., and DEKEYSER, J., 2003, J. Nucl. Mater., 320, 299.

SINGH, B.N., EDWARDS, D.J., and BILDE-SØRENSEN, J.B., 2004, Risø Report No. Risø-R-1485(EN), October 2004, p.29.

SINGH, B.N., EDWARDS, D.J., TÄHTINEN, S., 2004, Risø Report No. Risø-R-1436(EN), December 2004, p. 24.

ZINKLE, S.J., and GIBSON, L.T., 2000, Fusion Materials Semiannual Prog. Report for the Period Ending December 31, 1999, DOE/ER-0313/27, March 2000, p. 163.

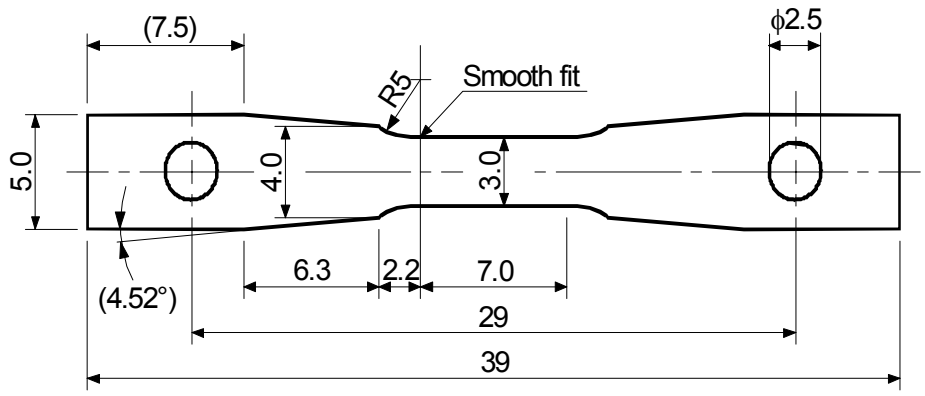

Figure 1. Size and geometry of tensile specimens used in the present investigations.

(a)

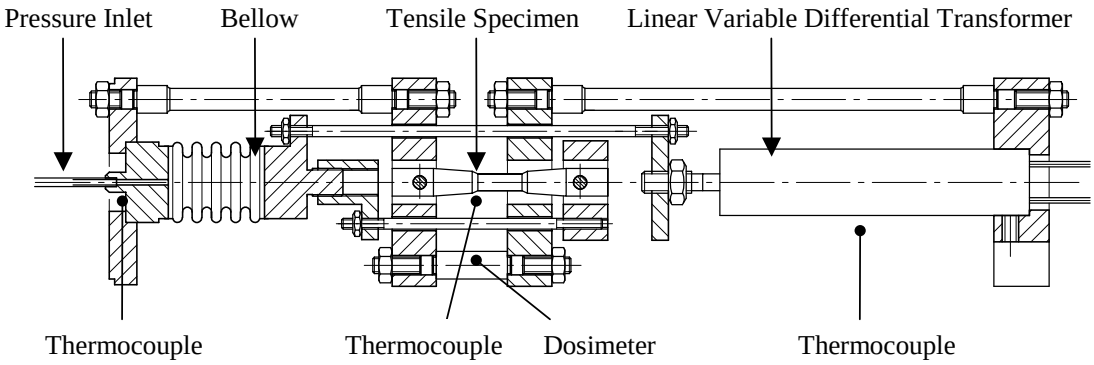

(b)

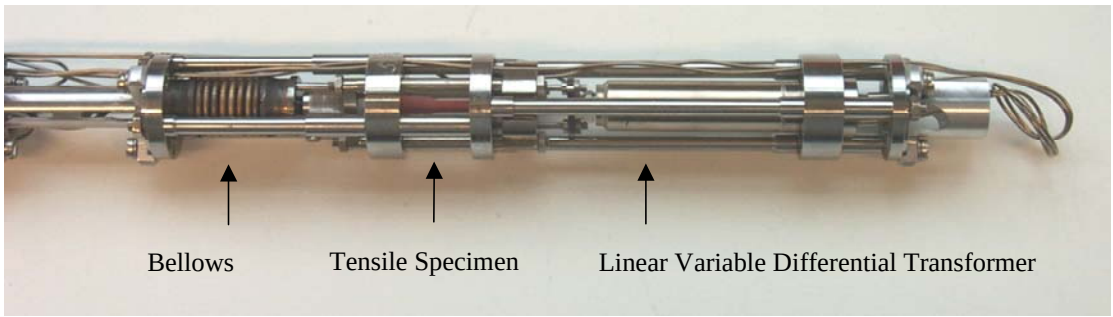

Figure 2. (a) Simplified layout and operational features of the test module used in the in-reactor tensile tests and (b) the final assembly of the complete test module in the instrumented irradiation rig.

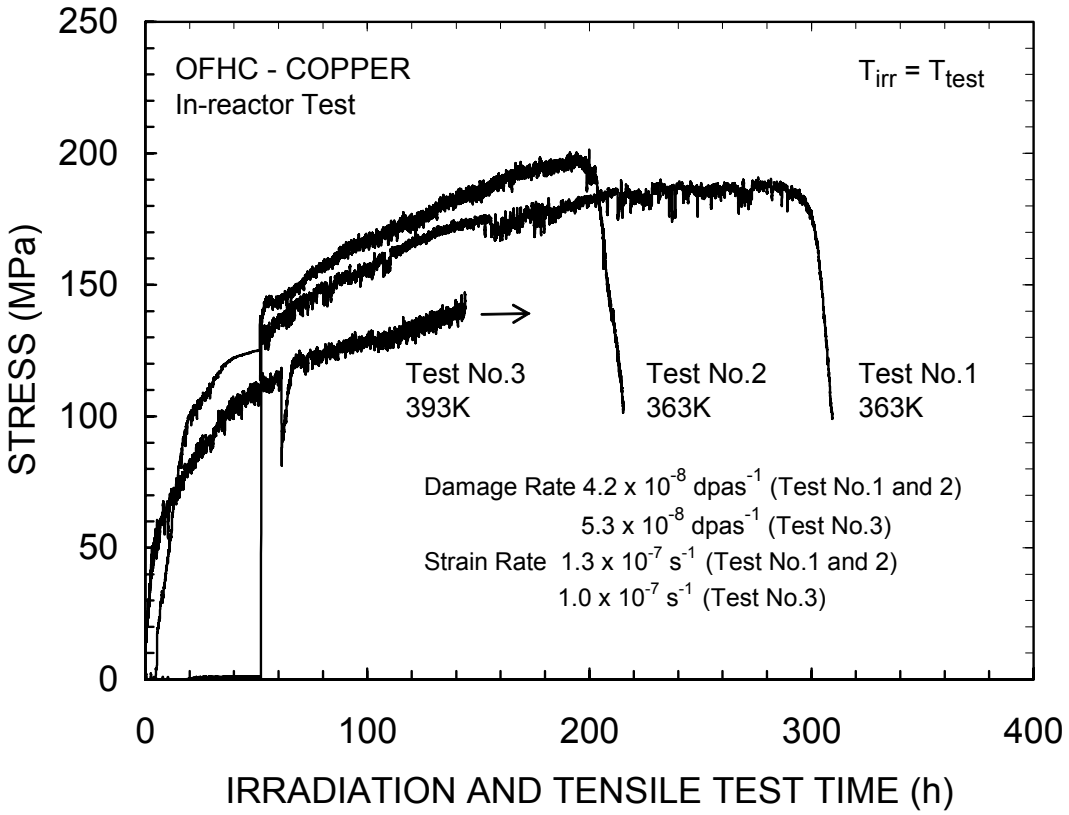

Figure 3. Continuously measured stress response as a function of irradiation and tensile test time during the in-reactor tensile tests. Note that the specimens in the Test No. 1, 2, 3 received different level of pre-loading displacement dose before the actual tensile test was activated and the specimens started experiencing applied stress. As a result, different amounts of irradiation-induced defects and their clusters accumulated during the pre-yield period in the absence of dislocation generation.

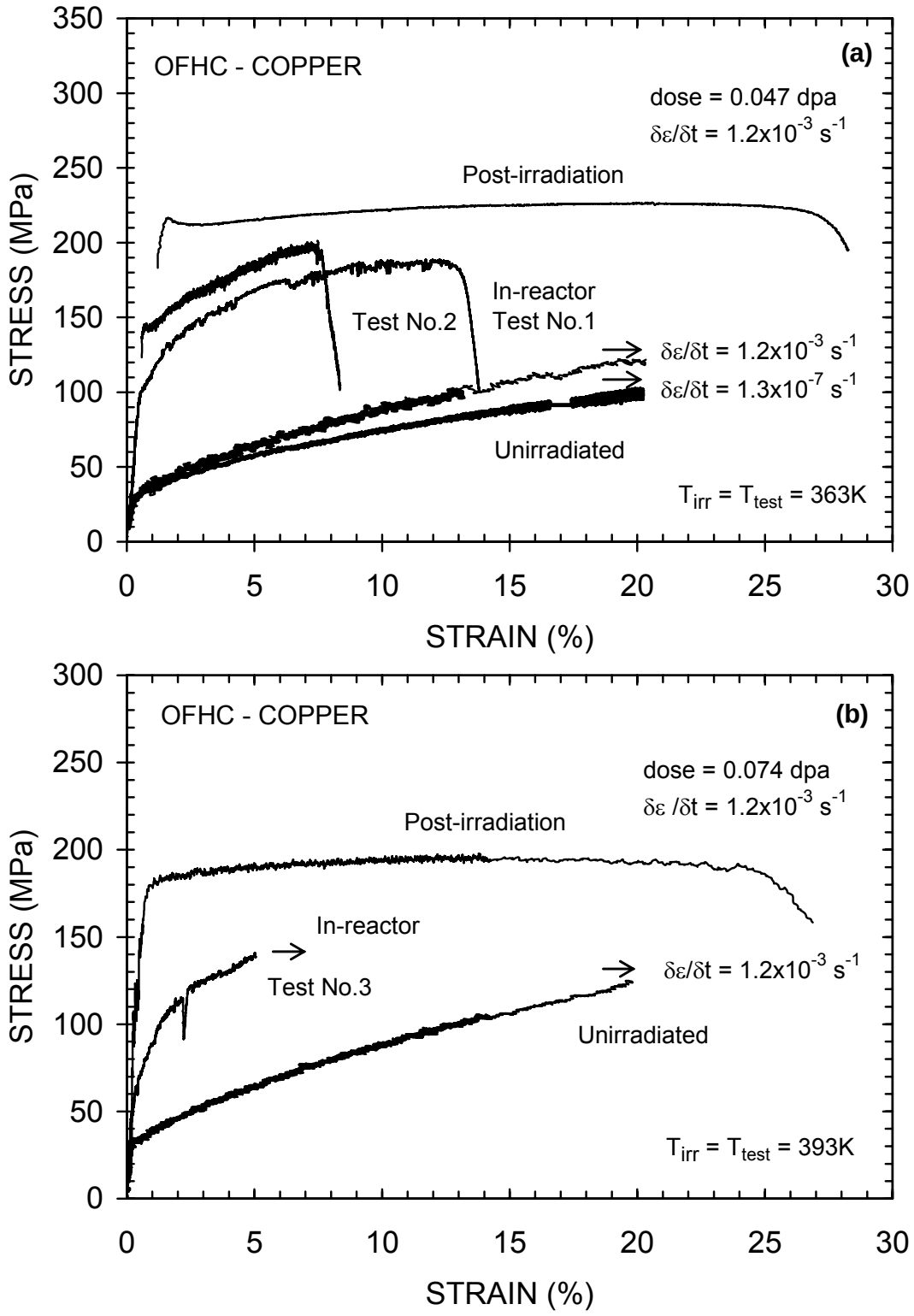

Figure 4. Engineering stress-strain curves for the in-reactor tensile tests carried out at (a) 363K and (b) 393K. For both cases, the curves for the post-irradiation and pre-irradiation tests carried out outside of the reactor are also shown. Note that in these in-reactor tests, the stress-strain curves represent the combined effects of strain hardening due to the applied stress and radiation hardening due to increasing level of displacement dose.

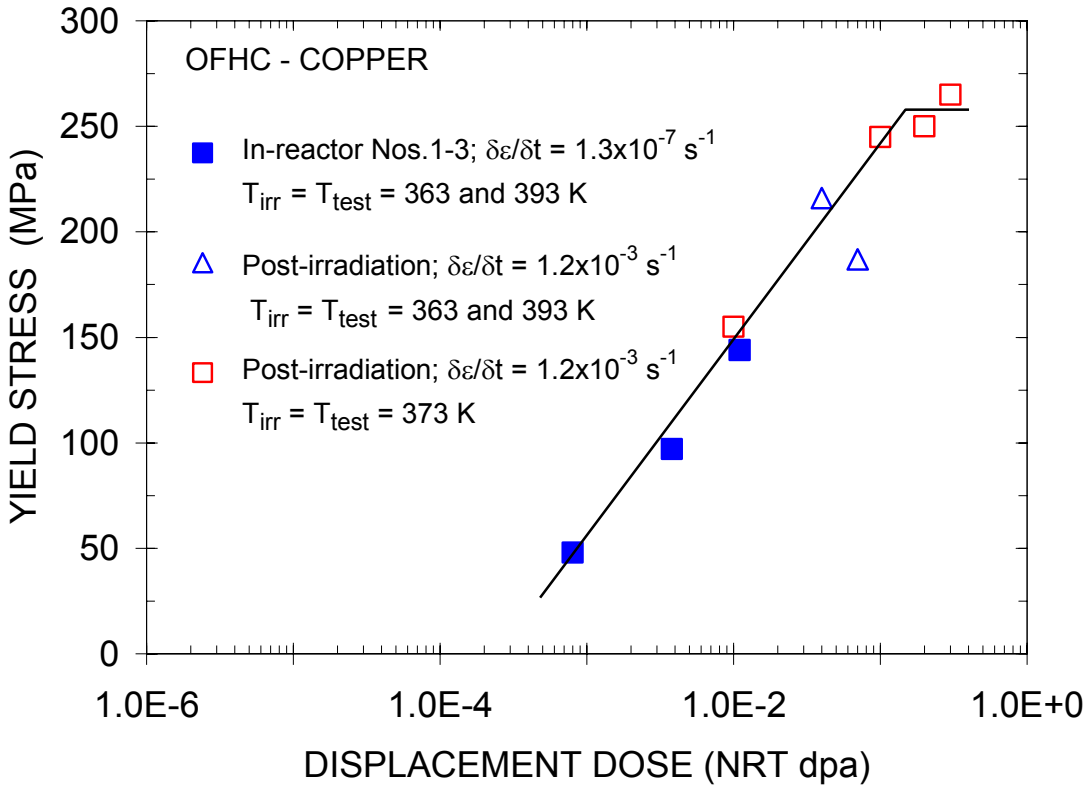

Figure 5. Displacement dose dependence of the yield stress for the in-reactor as well as post-irradiation tests at 363 – 393K. It is interesting to note that the dose dependence of the yield stress for the in-reactor rests and the post-irradiation tests is almost identical.

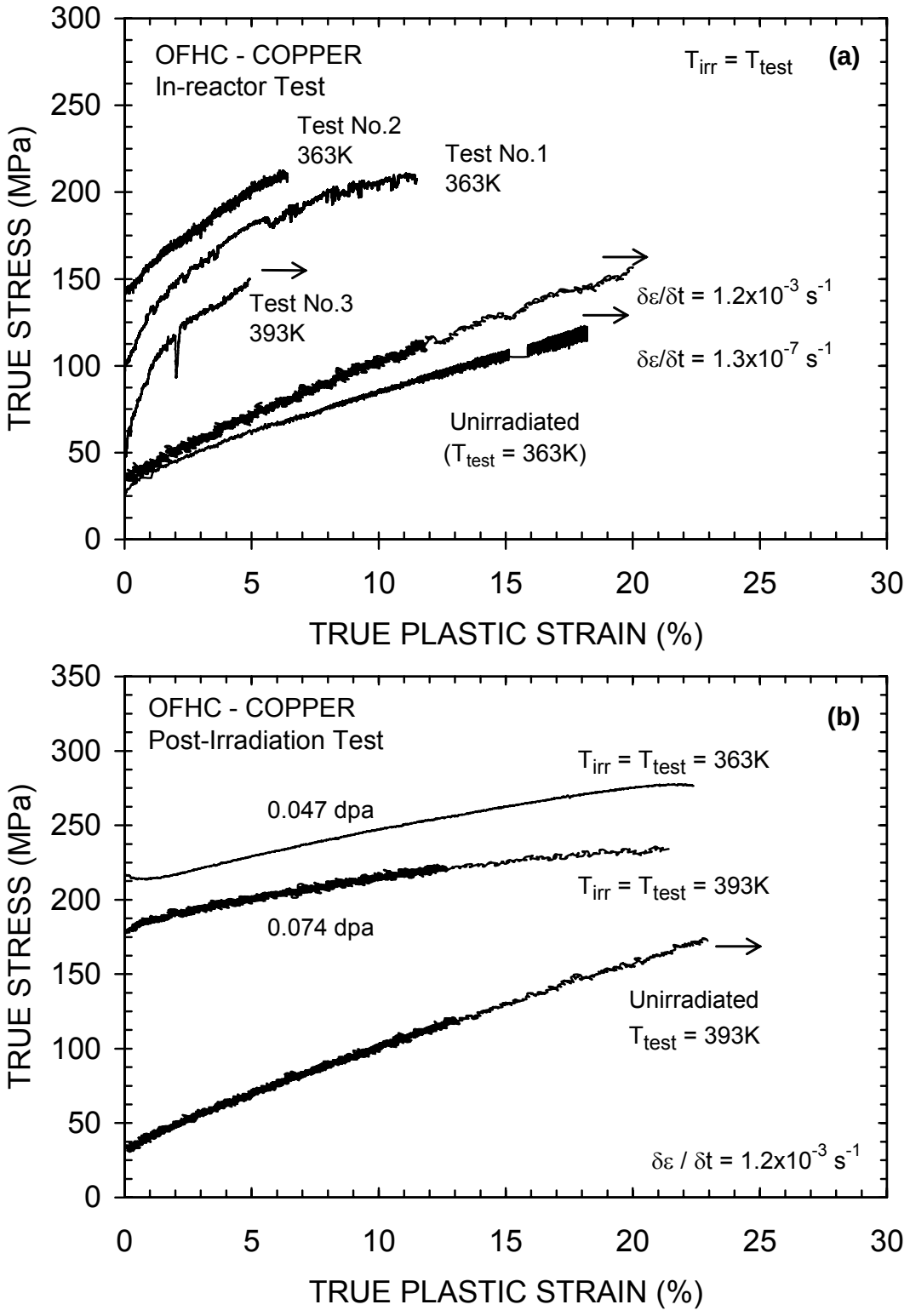

Figure 6. True stress – true strain curves for (a) the in-reactor tests and (b) the post-irradiation tests at 363 and 393 K. The corresponding curves for the unirradiated specimens are also shown. Note the difference in the hardening behaviour between the in-reactor tests and the post-irradiation tests.

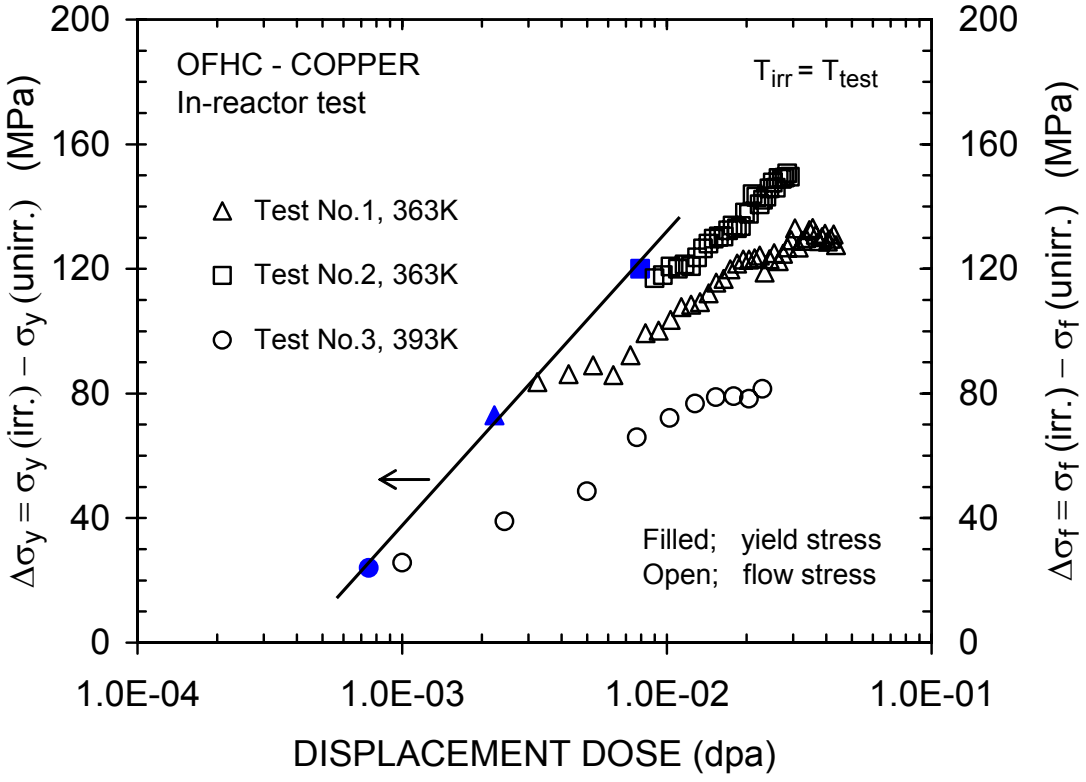

Figure 7. Irradiation induced increase in yield stress, $\Delta\sigma_y$, and flow stress, $\Delta\sigma_f$, as a function of displacement dose level for the in-reactor tensile tests at 363 and 393K. The following features are worth noting: (a) the increase in the yield stress with dose is faster than that of the flow stress, (b) the rate of flow stress increase tends to saturate at a certain dose level particularly when the pre-yield doe level is low (e.g. Test No. 1 and 3) and (c) the magnitude of the increase in the flow stress decreases substantially with decreasing the pre-yield dose level.

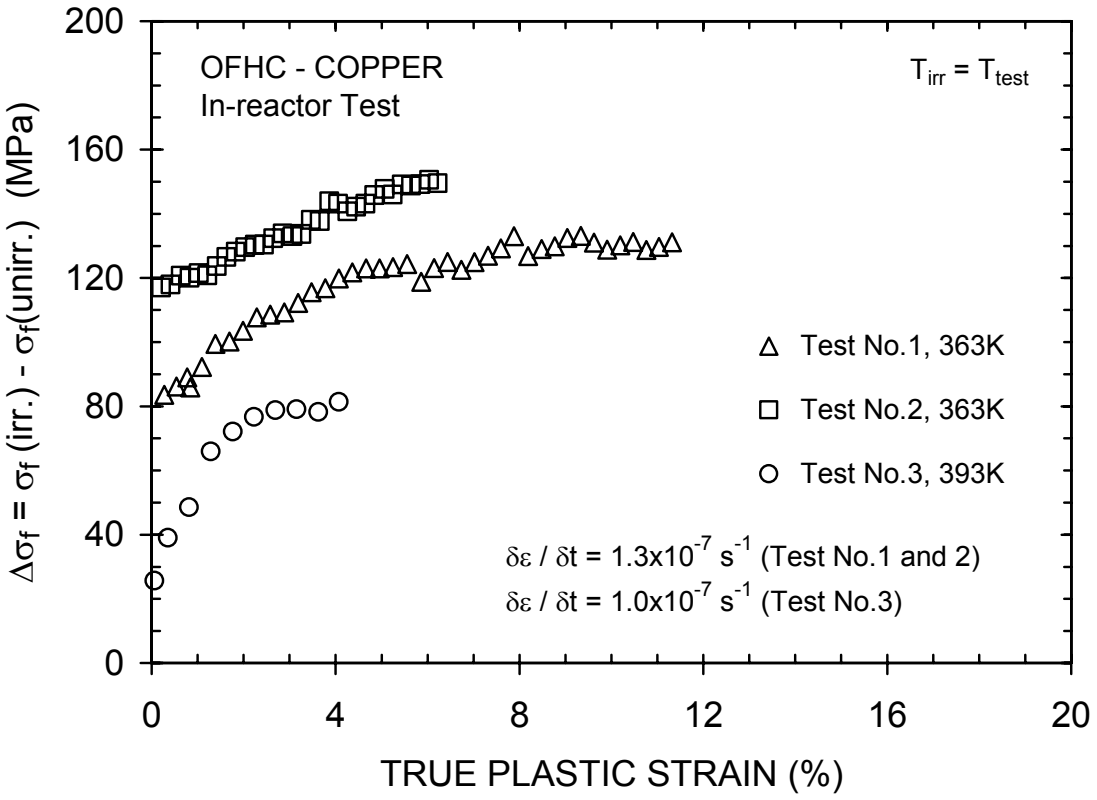

Figure 8. Increase in flow stress, $\Delta\sigma_f$, as a function of true plastic strain for in-reactor tests at 363 and 393K. Note that while the increase in the flow stress, $\Delta\sigma_f$, decreases with strain, the magnitude of the increase in the flow stress (at a given strain (dose) level) increases with increasing level of pre-yield displacement dose. Furthermore, the increase in the flow stress beyond a certain strain level (i.e. dose) decreases with increasing strain (dose) and then tends to saturate (e.g. Test No. 1 and 3).

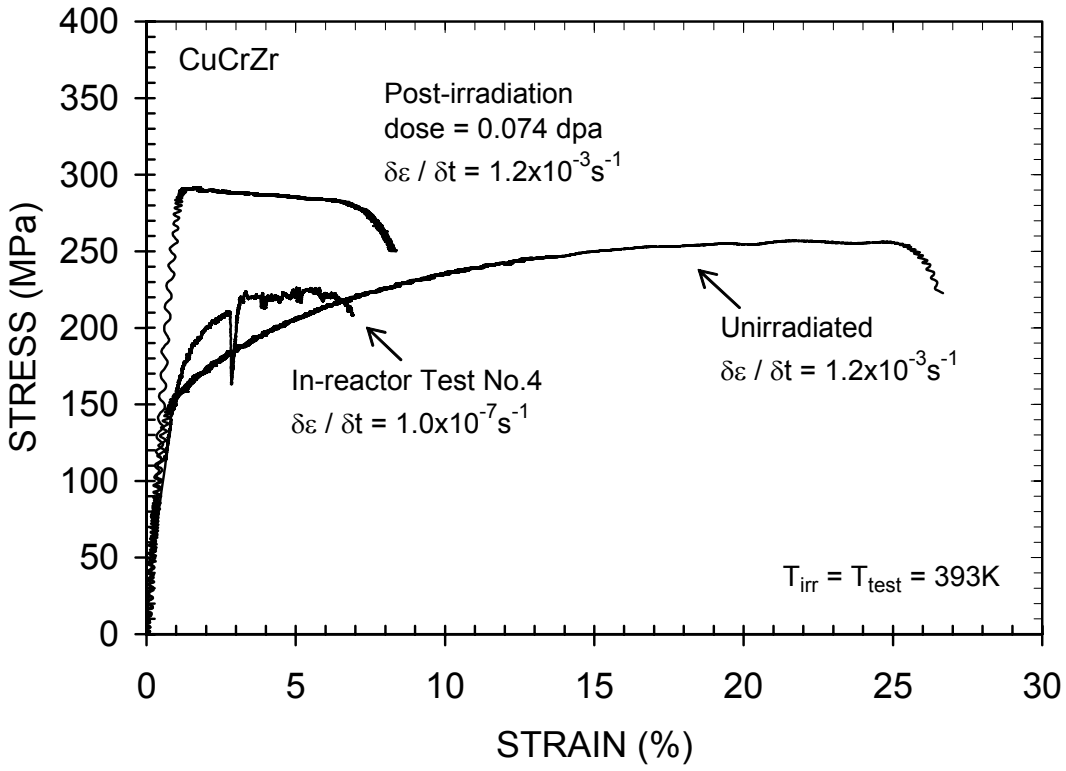

Figure 9. Stress-strain curves for the prime aged CuCrZr alloy at 393K obtained during the in-reactor test (Test No. 4). For comparison, the results for the out-of-pile tests on the unirradiated and post-irradiated (0.074 dpa) CuCrZr specimens are also shown. Note that the in-reactor test was terminated already at a dose level of ~ 0.037 dpa because of the onset of fracture.

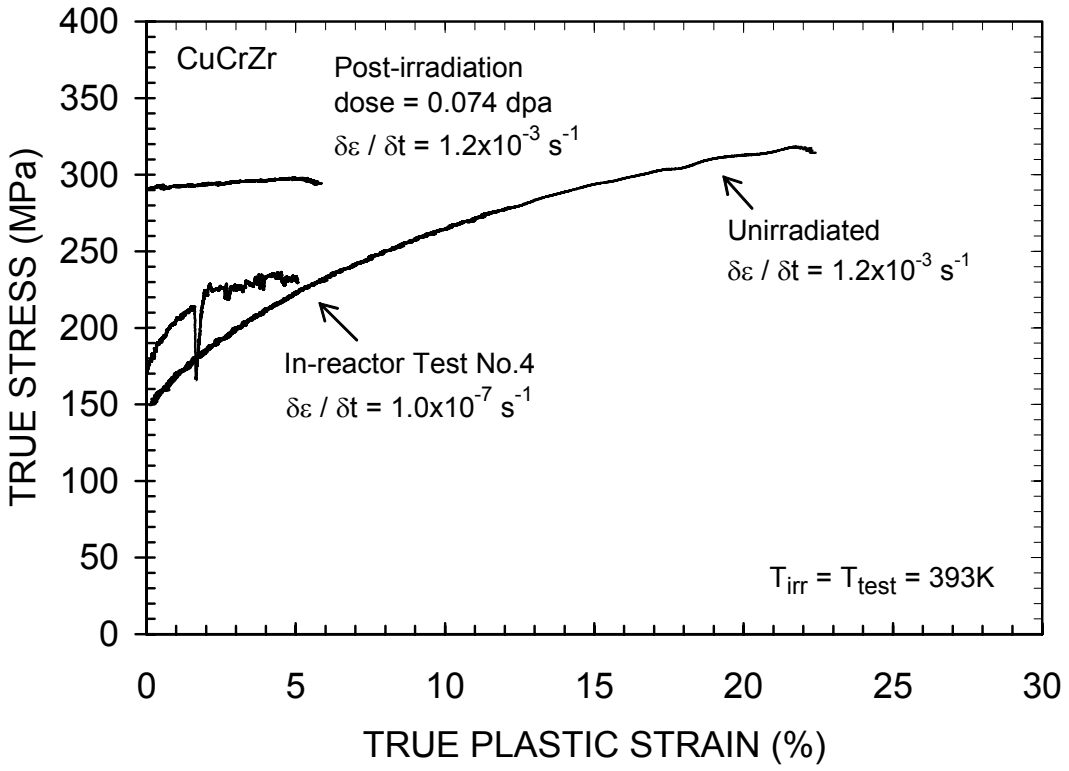

Figure 10. True stress - true strain curves for the CuCrZr alloy corresponding to the engineering stress-strain curves shown in figure 9.

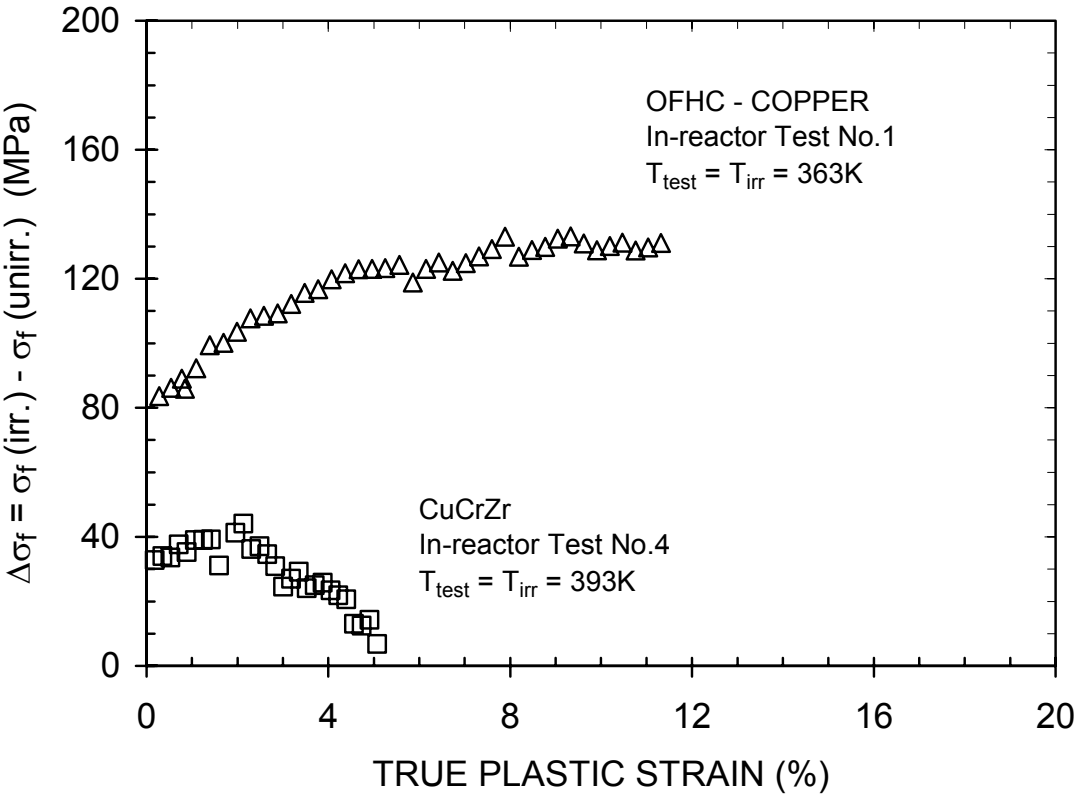

Figure 11. The irradiation-induced increase in the flow stress, $\Delta\sigma_f$, as a function of true plastic strain for the in-reactor test (Test No. 4) on CuCrZr alloy at 393K and the corresponding post-irradiation test carried out also at 393K. Note the difference in the strain rates between the in-reactor and the post-irradiation tests. For comparison the variation of $\Delta\sigma_f$ with strain for OFHC-copper tested at 363K (Test No. 1) is also shown. The dose level of the yield point was very similar in these two tests (see Table 1).

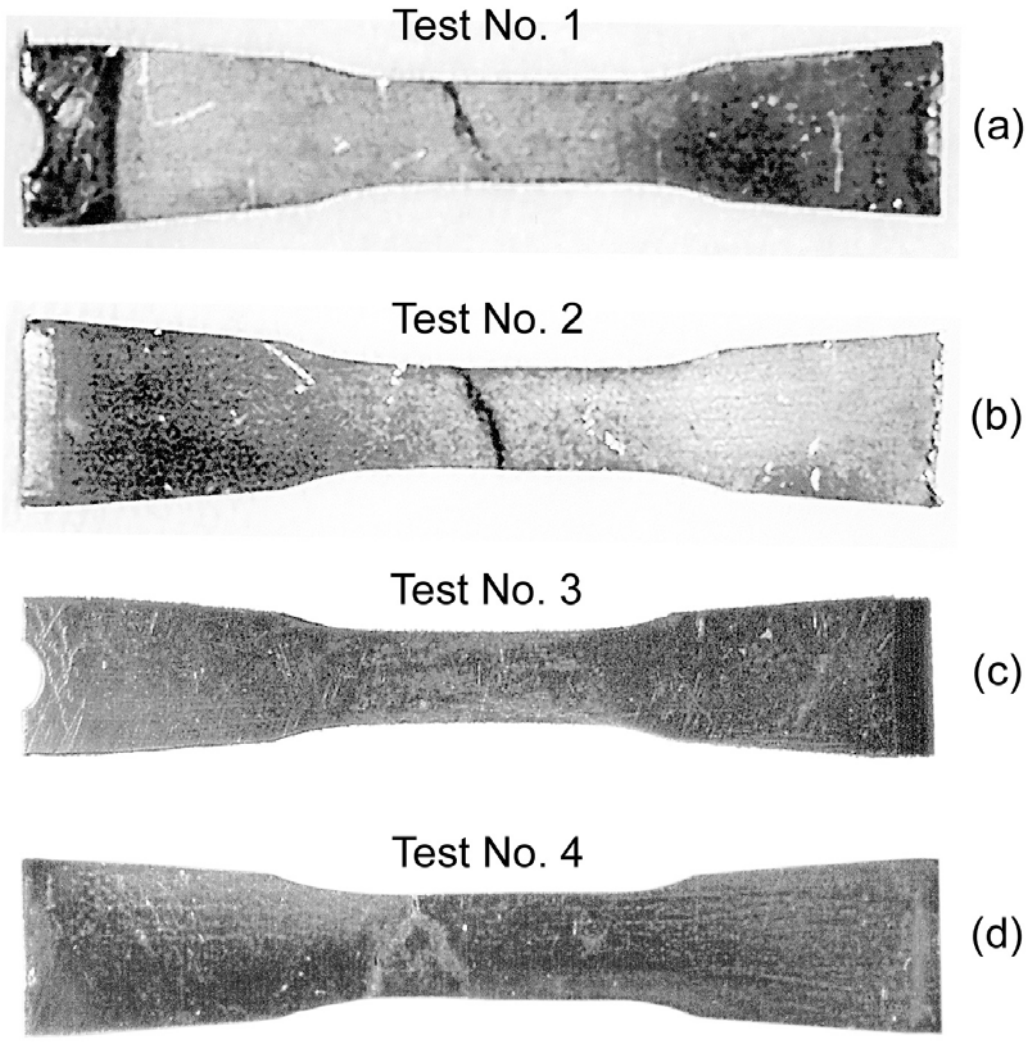

Figure 12. Photographs of tensile specimens after in-reactor tests showing crack formation in specimens used in Test No. 1, 2 and 4. The specimen used in the Test No. 3 shows no indication of any crack formation even though the specimen yielded the highest uniform elongation and experienced the highest dose level compared to specimens in Tests No. 1, 2 and 4 (see Table 1).

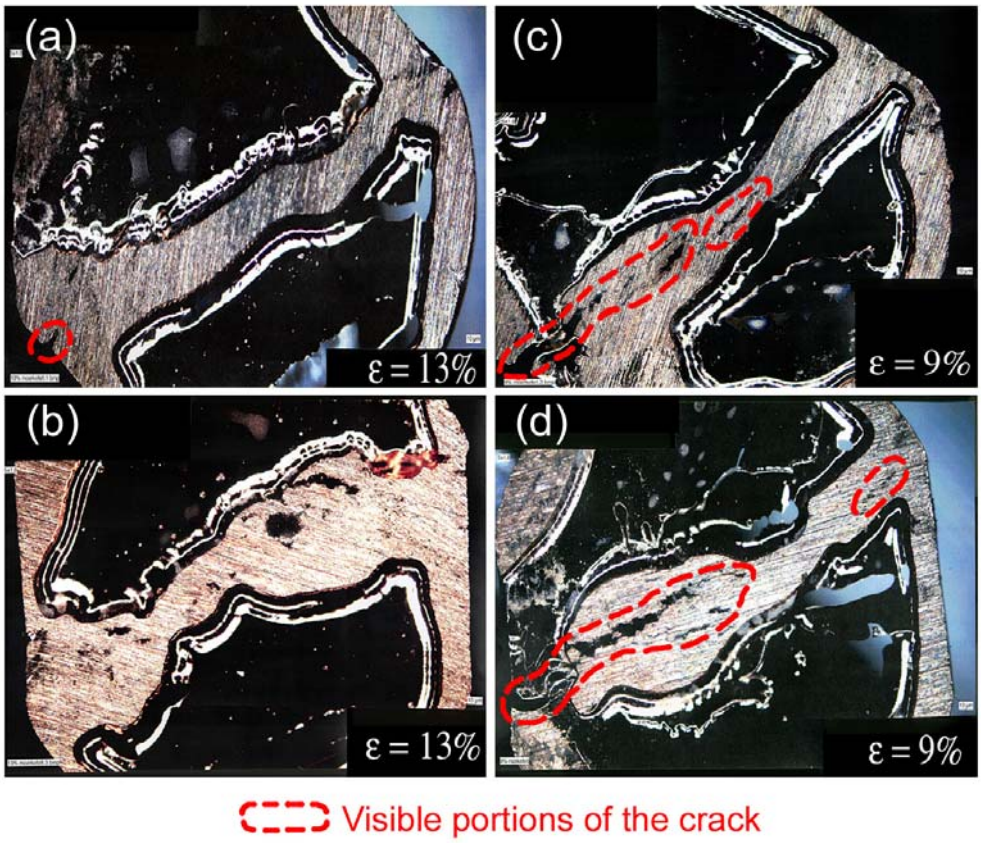

Figure 13. Optical micrographs of both sides of the cracked portion of the gauge width of the tensile specimens used in Test No. 1 and 2 (see figures 12(a) and 12(b). Note that there is no sign of the presence of any crack on either side of the specimen from the Test No. 1 (figures 13a, b) showing that the crack did not propagate through the whole thickness of this specimen. In the case of the specimen from the Test No. 2, on the other hand, certain portions of the crack has indeed propagated through the whole thickness (figures 13c, d) of the specimen.

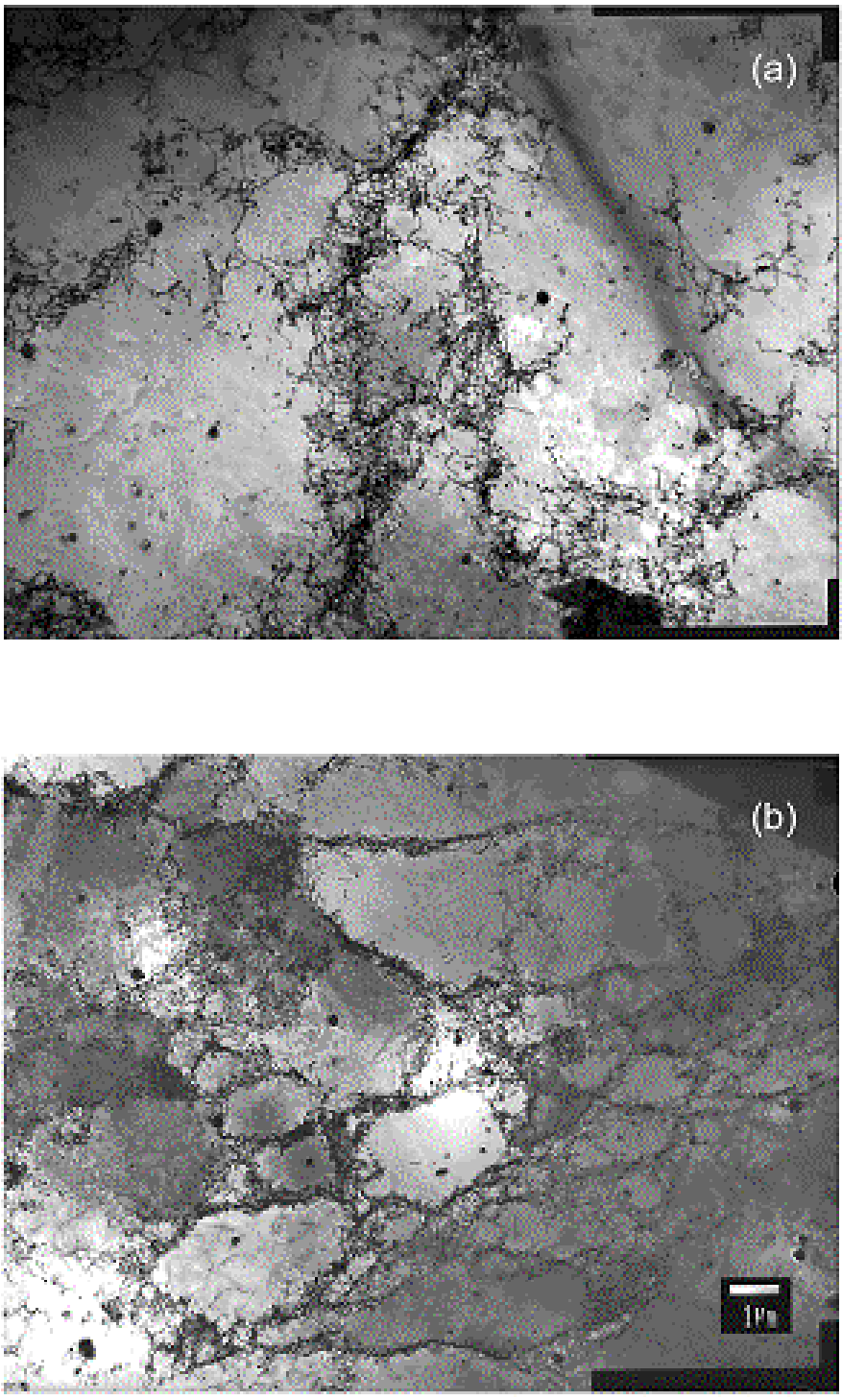

Figure 14. Dislocation microstructure in the unirradiated copper specimens tensile tested at 363K and at a strain rate of 1.3 x 10^{-7} s^{-1} to a total strain of (a) 4% and (b) 20%. Note the segregation of dislocations and the formation of dislocation cells.

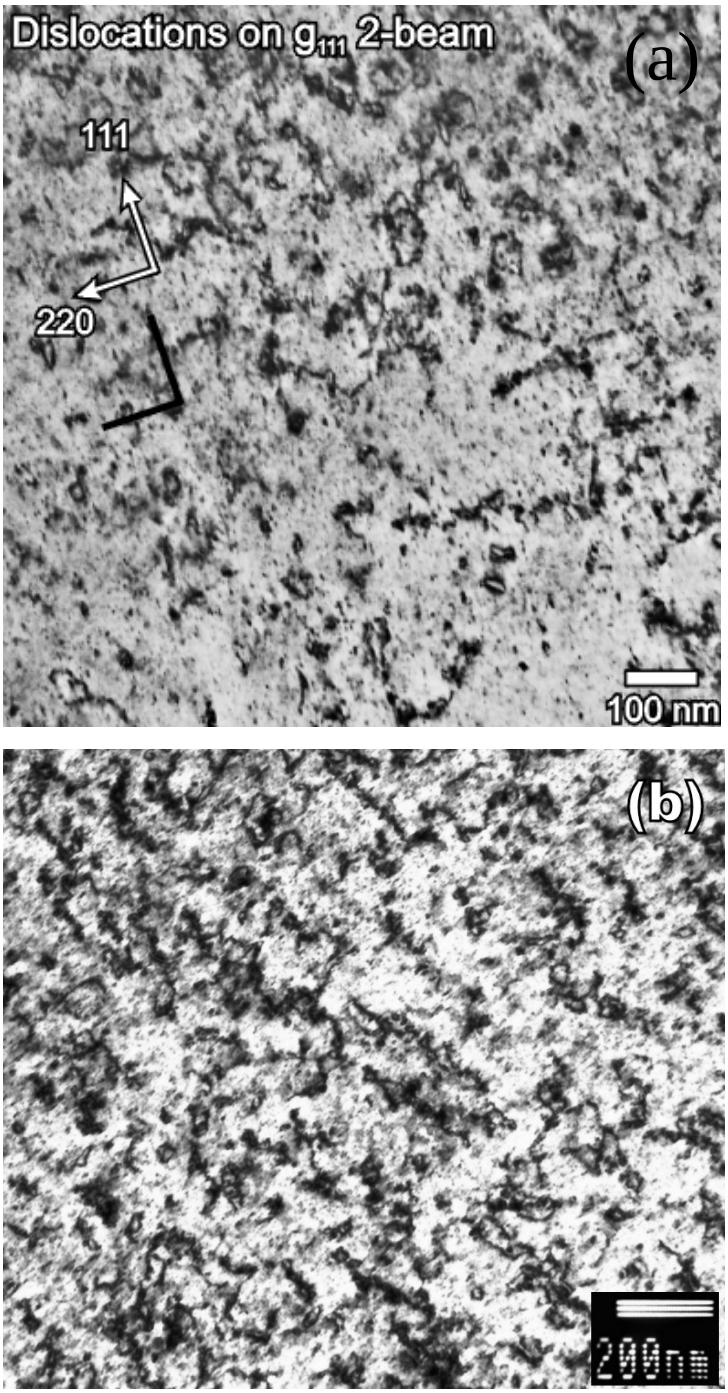

Figure 15. Microstructure in the as-irradiated "reference" specimens (but without stress) corresponding to (a) Test No. 1 (at 363K) and (b) Test No. 3 (at 393K) to final displacement doses of 0.047 and 0.074 dpa, respectively. The microstructure is characterized by the presence of black dots, small loops and raft-like structure of loops. The clusters of vacancies in the form of SFTs are not visible in these micrographs.

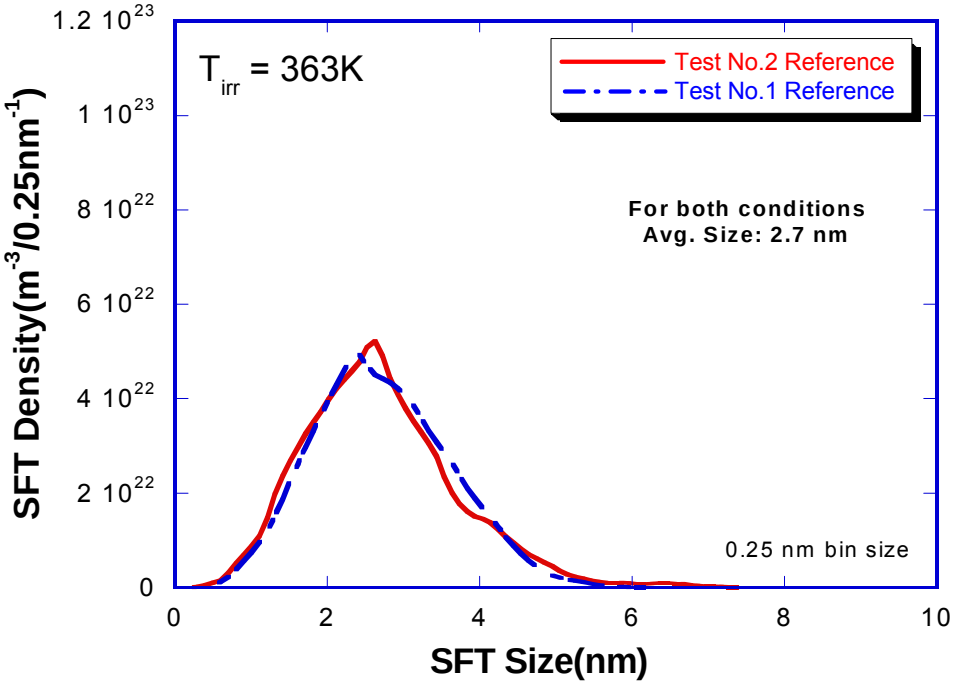

Figure 16. Size distributions of SFTs in the "reference" tensile specimens (without stress) corresponding to the in-reactor Test No. 1 and 2. Note that the size distributions are almost identical and are also similar to the ones reported earlier for the irradiation temperature of 373K (Singh et al. 2001).

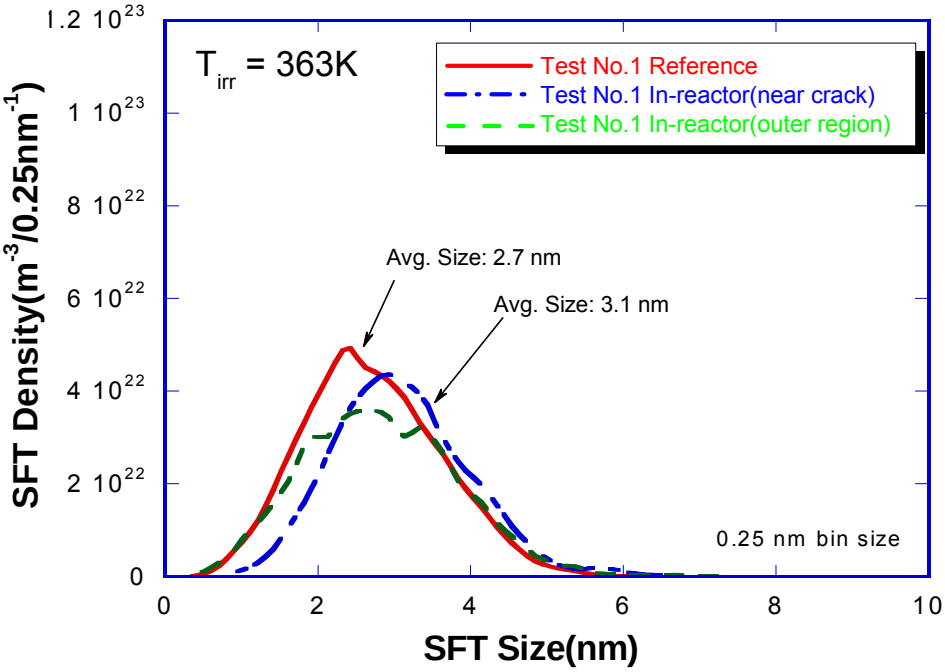

Figure 17. Size distributions of SFTs in the in-reactor tensile tested specimens in Test No. 1. For comparison, the size distributions for the "reference" specimens are also shown. Note the difference in the size distributions between the "reference" specimens and the in-reactor deformed specimen showing a significant decrease in the density of smaller SFTs in the in-reactor deformed specimen. The size distribution in the region away from the crack and the gauge length (i.e. "outer region" where practically no plastic deformation has occurred) is very similar to the one for the undeformed reference specimen.

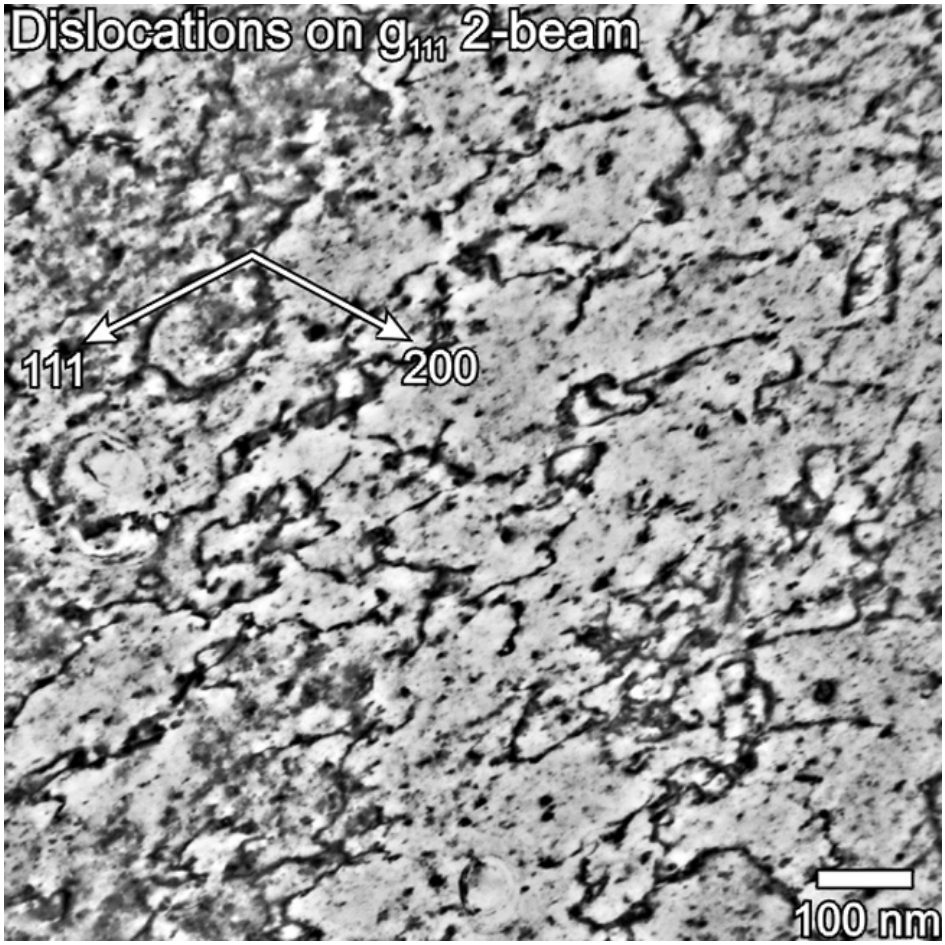

Figure 18. An example of the dislocation microstructure in the in-reactor deformed specimen in the Test No. 1 at 363K. Note the homogeneous nature of spatial distribution of deformation induced dislocations and an almost complete lack of dislocation segregation in the form of dislocation walls.

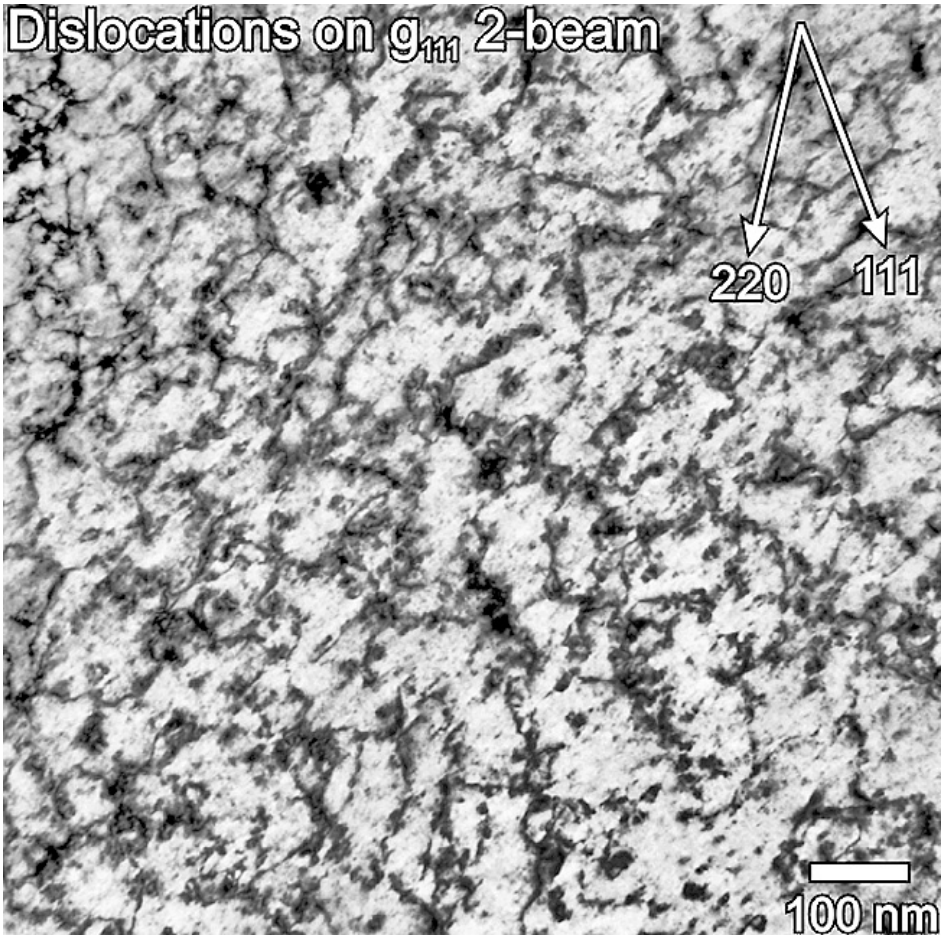

Figure 19. An example of the dislocation microstructure in the in-reactor deformed specimen at 363K (Test No. 2) with a pre-loading dose level of ~0.01 dpa. Like in the case of the Test No. 1 (figure 18), dislocations are homogeneously distributed and there is no indication of any extensive amount of dislocation-dislocation interactions and formation of dislocation walls.

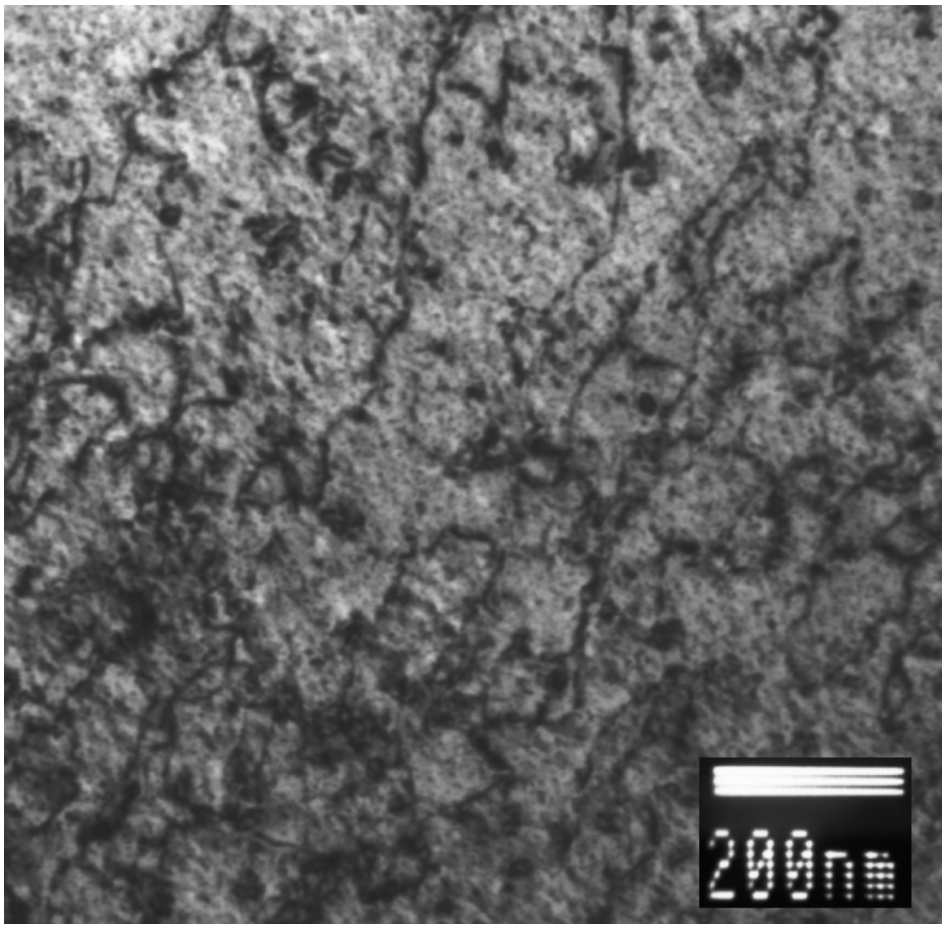

Figure 20. Dislocation microstructure in the in-reactor deformed specimen (Test No. 3) at 393K. The main features of the microstructure are very similar to those in figures 18 and 19.

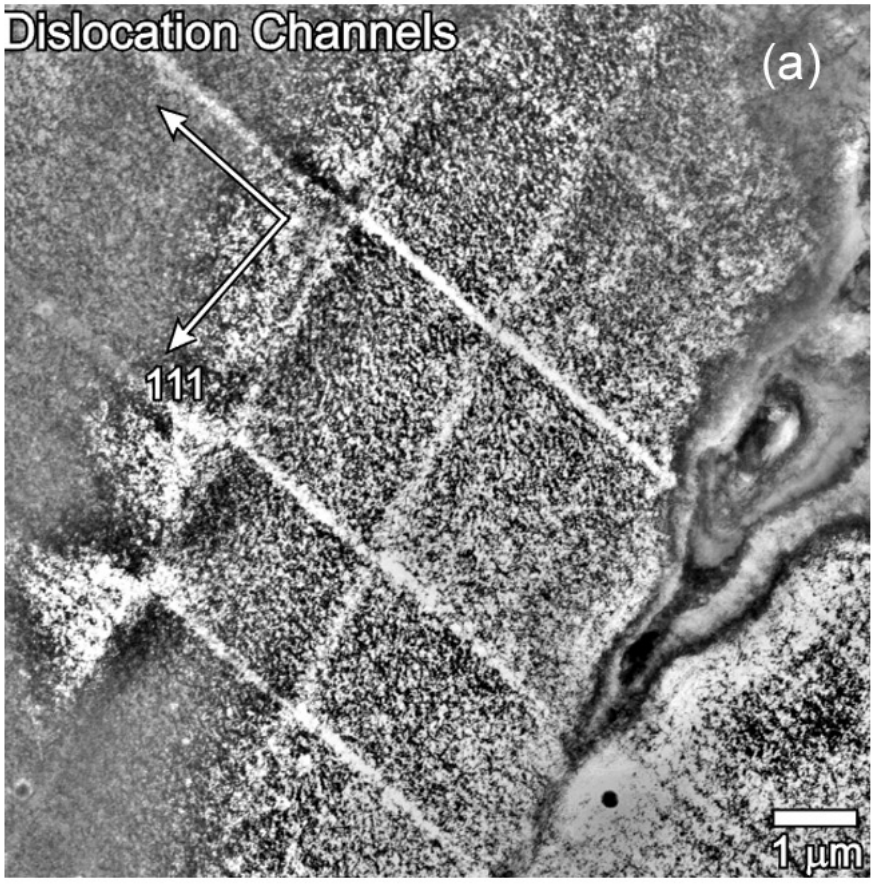
Dislocation Channels
(a)
111
1 µm

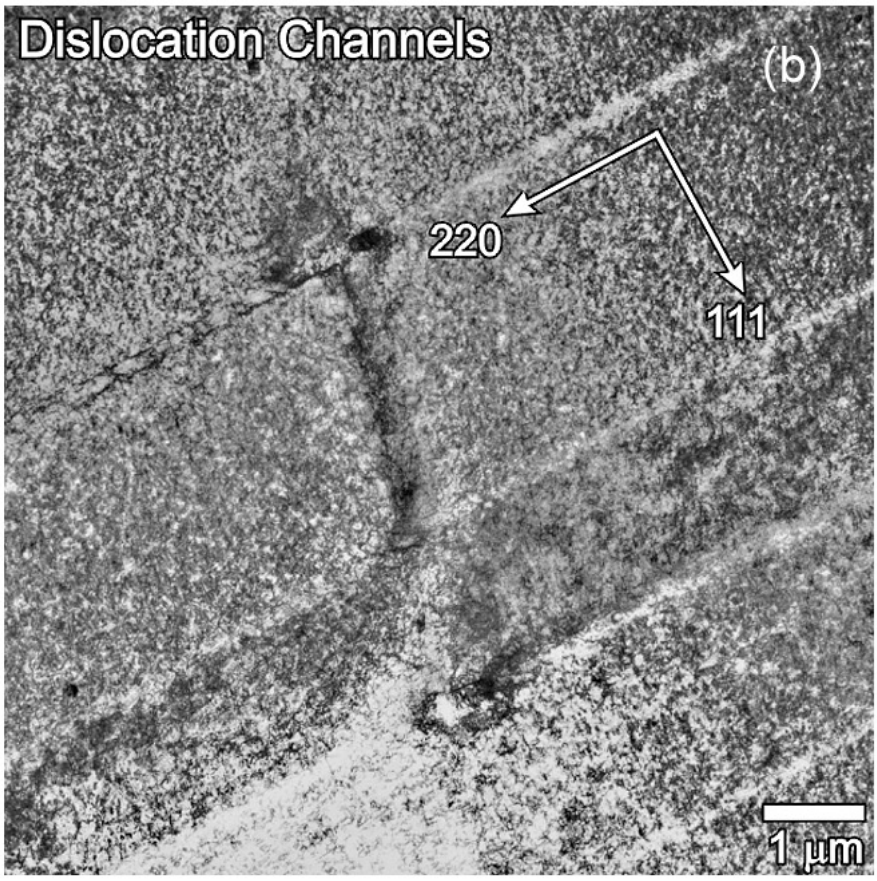
Dislocation Channels
(b)
220
111
1 µm

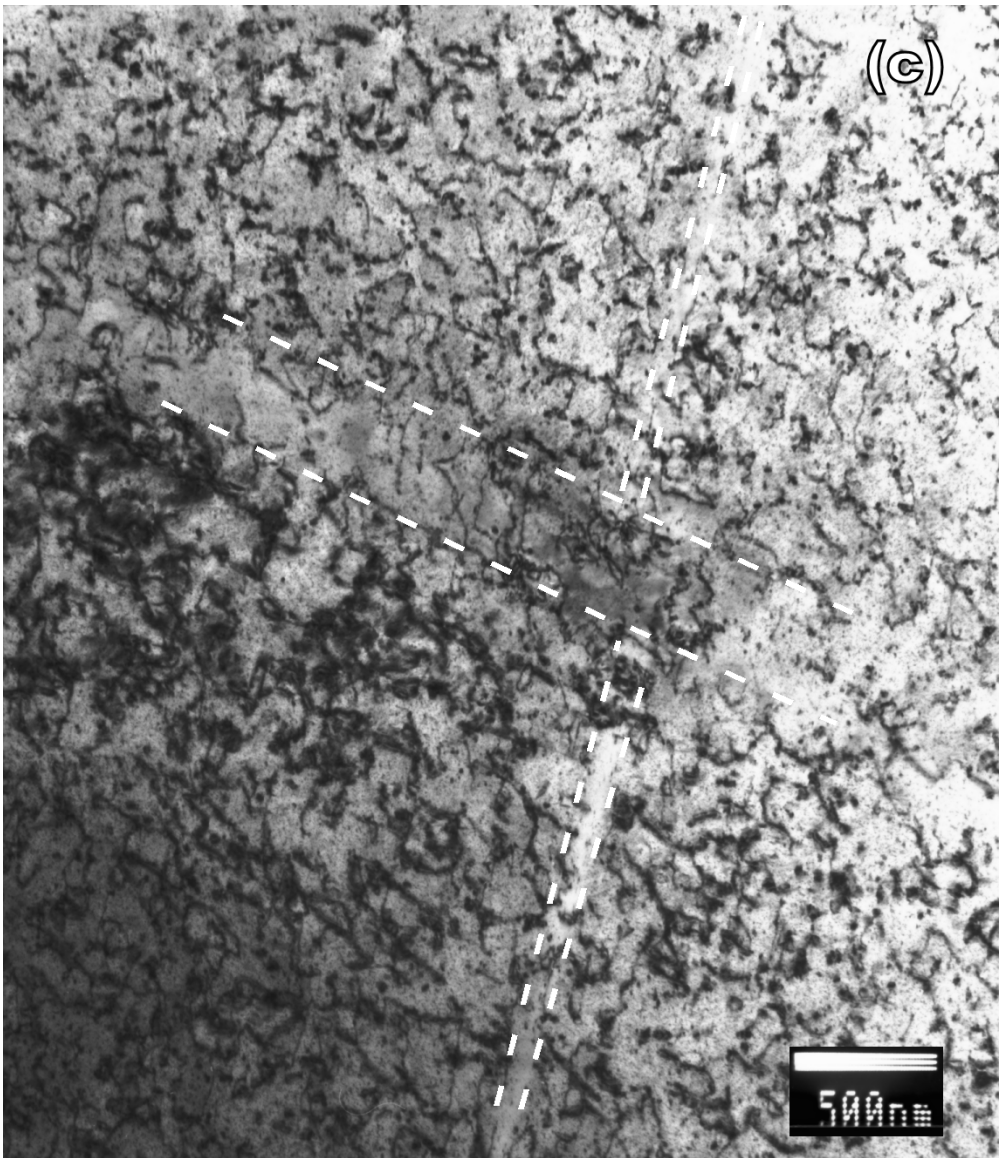

Figure 21. Examples of cleared channels observed in the specimens deformed in the in-reactor tensile tests (a) Test No. 1, (b) Test No. 2 and (c) Test No. 3.

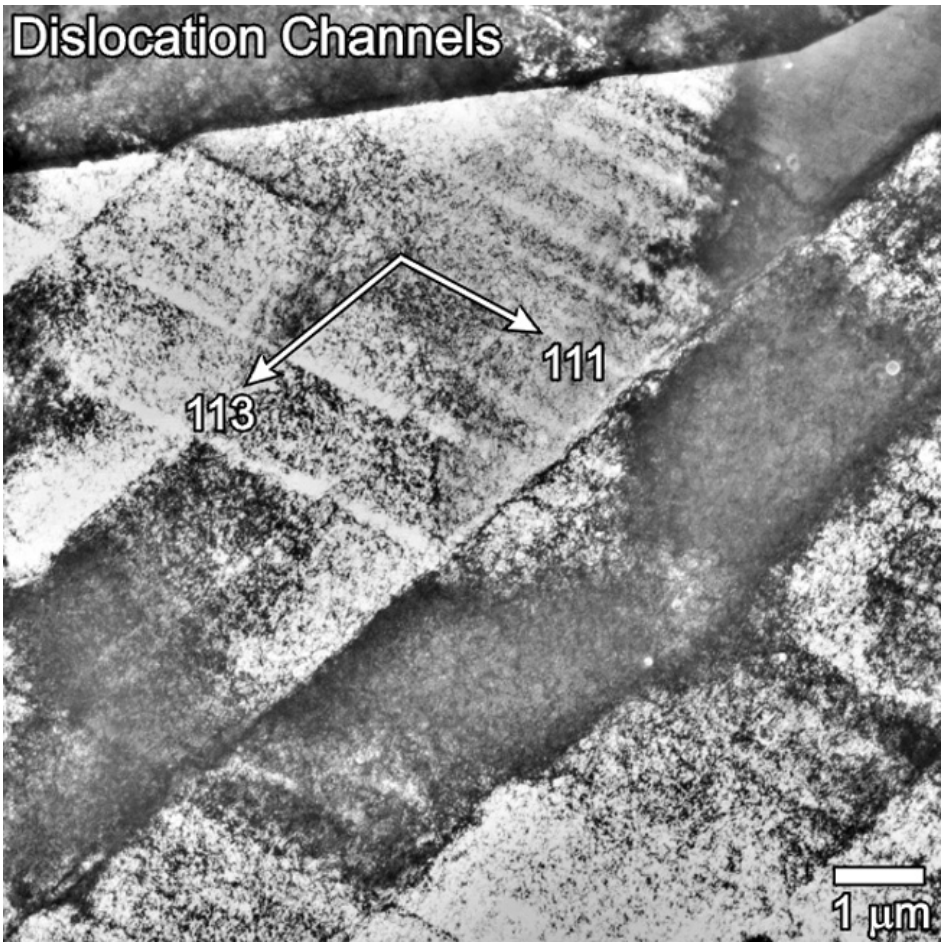

Figure 22. An example of the initiation of cleared channels from a twin boundary in the specimen from Test No. 1 irradiated to a final dose level of ~0.047 dpa at 363K. The channels are initiated at one twin boundary, propagate across the twin and end at the other twin boundary. The channels are not transmitted into the neighbouring grain and remained confined within the twin. Similar examples have been reported for copper irradiated and tested at 373K to a dose level of 0.3 dpa (Singh et al. 2004).

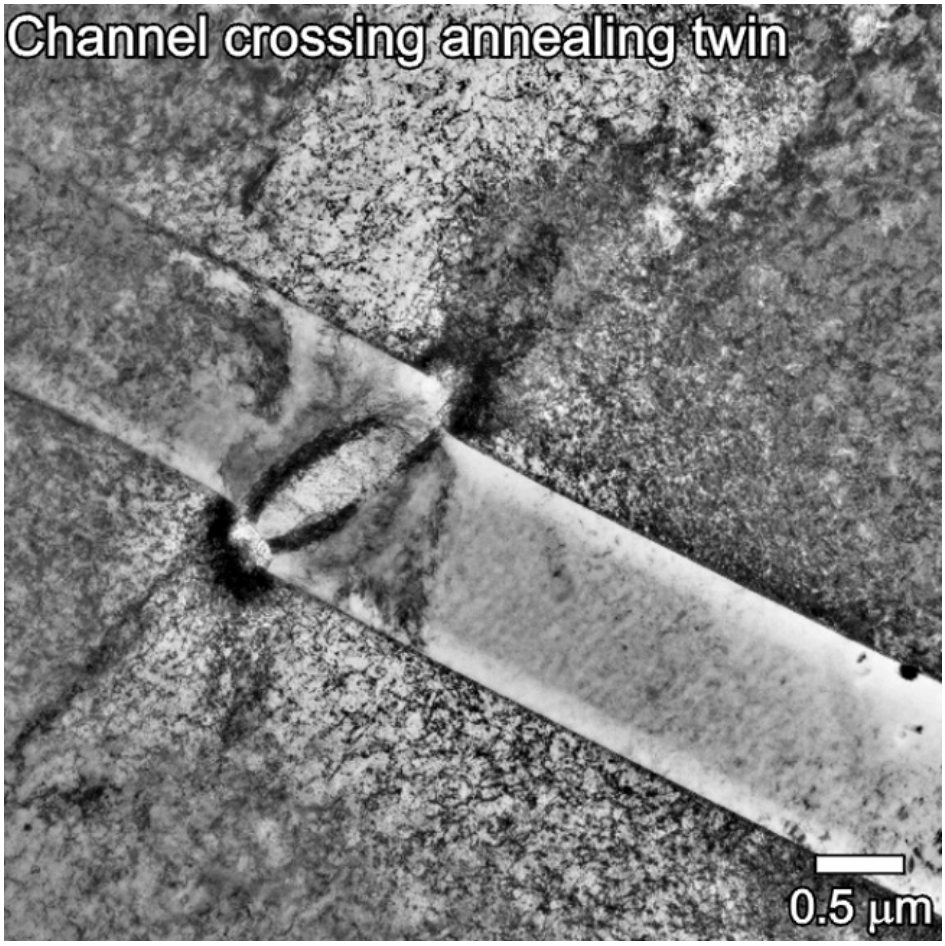

Figure 23. Interaction and propagation of a cleared channel across an annealing twin in the specimen from the in-reactor Test No. 2. Note that the annealing twin is badly damaged both at entry and the exit points of the cleared channel (see Singh et al. 2004 for such examples for post-irradiation tests).

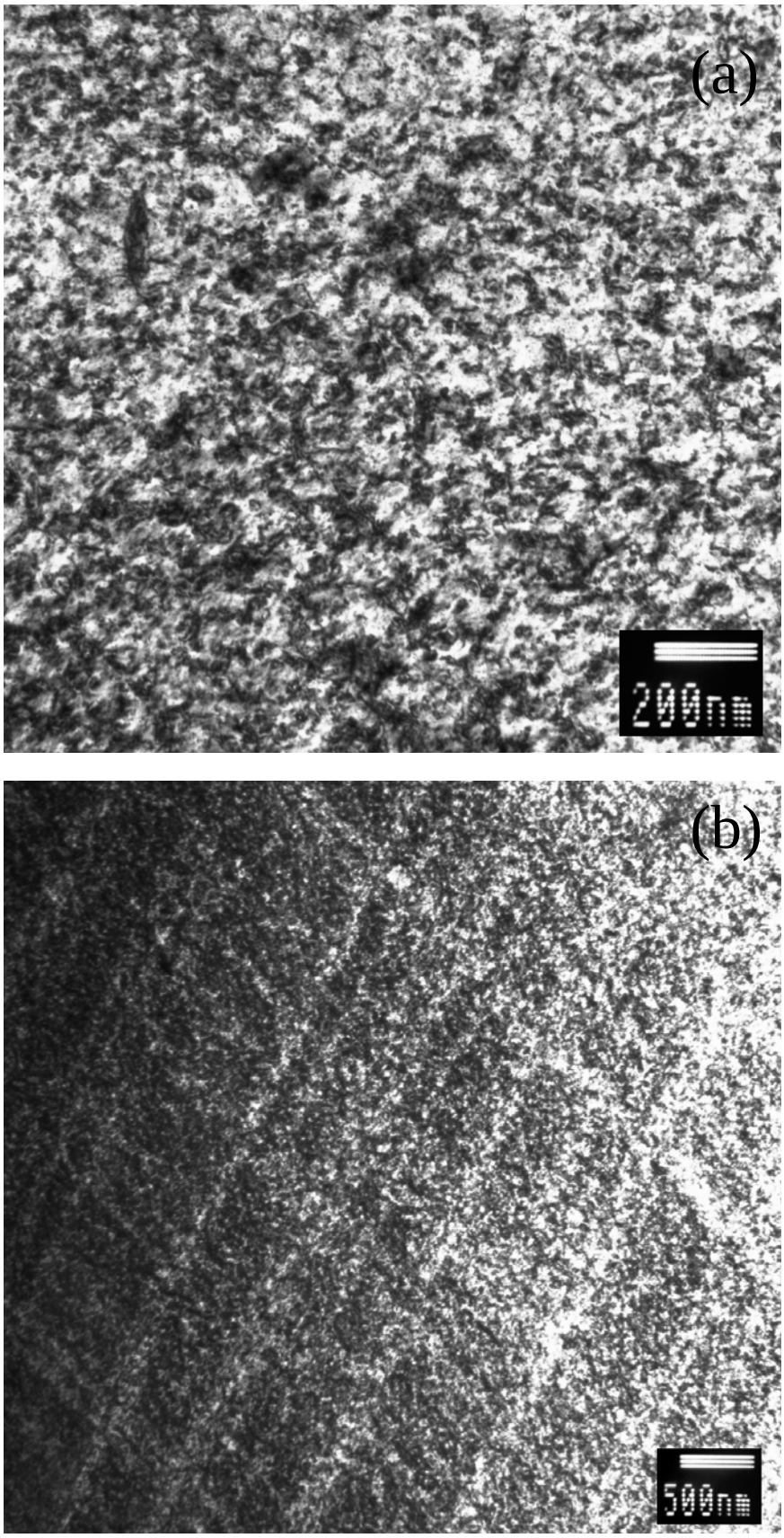

Figure 24. Microstructure of CuCrZr specimen deformed in the in-reactor test (Test No. 4) at 393K showing (a) defect clusters and dislocations and (b) cleared channels. Note the high density of cleared channels.

Mission

To promote an innovative and environmentally sustainable technological development within the areas of energy, industrial technology and bioproduction through research, innovation and advisory services.

Vision

Risø's research **shall extend the boundaries** for the understanding of nature's processes and interactions right down to the molecular nanoscale.

The results obtained shall **set new trends** for the development of sustainable technologies within the fields of energy, industrial technology and biotechnology.

The efforts made **shall benefit** Danish society and lead to the development of new multi-billion industries.